



## Investigation of a model predictive control (MPC) strategy for seasonal thermochemical energy storage systems in district heating networks

Zhichen Wei<sup>a,b,\*</sup>, Paige Wenbin Tien<sup>a</sup>, John Calautit<sup>a</sup>, Jo Darkwa<sup>a</sup>, Mark Worall<sup>a</sup>, Rabah Boukhanouf<sup>a</sup>

<sup>a</sup> Department of Architecture and Built Environment, University of Nottingham, UK

<sup>b</sup> School of Automation, Guangxi University of Science and Technology, Liuzhou 545006, China

### HIGHLIGHTS

- Implemented model predictive control (MPC) strategy for seasonal thermal energy storage (STES).
- MPC strategy simulated in a real-world district heating (DH) system in the UK.
- Used SVR, regression tree, and LSTM models for heating demand forecasting in MPC.
- Achieved high predictive accuracy with LSTM for 12-h ahead forecasting.
- MPC controlled thermochemical storage system stored all the waste heat to and reduced unmet demand to 15% at 80% supply.

### ARTICLE INFO

#### Keywords:

Seasonal thermal energy storage  
Demand response  
Model predictive control (MPC)  
District heating system  
Long short-term memory (LSTM)  
Thermochemical energy storage systems (STES)  
Support vector regression (SVR)  
Regression trees  
Built environment  
Machine learning

### ABSTRACT

This research investigates the integration of model predictive control (MPC) with seasonal thermochemical energy storage systems (STES) within district heating networks, focusing on the Nottingham district heating as a case study. The primary aim is to develop an MPC strategy that utilizes machine learning models for accurate heat load forecasting. This strategy optimizes the charging and discharging cycles of thermochemical energy storage systems to mitigate the mismatch between heating energy supply and demand by storing surplus heat during summer and utilizing it during winter. We employed and validated machine learning models, including support vector regression (SVR), regression trees, and long short-term memory (LSTM) networks, using historical heat load and meteorological data. A validated numerical model of the thermochemical energy storage system (TCES) was integrated into the MPC framework, formulated as a mixed-integer linear program to optimize the STES's operations. The performance of the MPC strategy was benchmarked against a rule-based control approach under varying supply capacities to evaluate scalability and robustness. Our findings reveal that each machine learning model achieved comparable performance, with CVRMSE values within the 9–11% range. The LSTM model, in particular, provided accurate multi-step forecasts essential for the MPC framework. Incorporating these models into the MPC strategy allowed for precise heat demand predictions, enhancing the management of energy storage and distribution. Results confirmed that MPC effectively shifts energy seasonally, reduces reliance on auxiliary heating during winter, and minimizes waste heat. The MPC strategy outperformed the rule-based control by storing a significantly higher percentage of waste heat and meeting a greater portion of the additional heat demand that was not covered by the auxiliary heat supply. The system demonstrated effective performance under varying supply capacities, with the MPC strategy efficiently utilizing stored heat to meet demand at 80% supply capacity, achieving a waste heat reduction to 4% and meeting most of the heat demand. However, performance declined at 60% capacity, indicating the need for careful consideration of supply capacities in system design. This study highlights the potential of integrating machine learning models with MPC to enhance the performance and adaptability of district heating systems with STES, minimizing waste heat and efficiently meeting energy demands.

\* Corresponding author at: Department of Architecture and Built Environment, University of Nottingham, UK

E-mail address: [Zhichen.Wei2@nottingham.ac.uk](mailto:Zhichen.Wei2@nottingham.ac.uk) (Z. Wei).

<https://doi.org/10.1016/j.apenergy.2024.124164>

Received 25 December 2023; Received in revised form 5 August 2024; Accepted 6 August 2024

Available online 21 August 2024

0306-2619/© 2024 The Authors. Published by Elsevier Ltd. This is an open access article under the CC BY license (<http://creativecommons.org/licenses/by/4.0/>).

Nomenclature		$\varphi$	Fraction of $\text{Co}_3\text{O}_4$ in total solid material
<i>Symbols</i>		$\emptyset$	Thermodynamic properties of solid material
A	System matrix in state space model	<i>Abbreviations</i>	
$A_s$	Solid cross section area ( $m^2$ )	CHP	Combined heat and power
$A_f$	Air flow area ( $m^2$ )	COP	Coefficient of performance
$A_c$	Total heat transfer area ( $m^2$ )	CVRMSE	Coefficient of variation of root mean square error
B	System matrix in state space model	DH	District heating
C	Concentration of reactants (mole/m)	EfW	Energy-from-waste
$f_h$	Hidden layer activation function	LSTM	Long short-term memory
h	Convective heat transfer coefficient ( $Wm^{-2}K^{-1}$ )	MAE	Mean absolute error
m	Mass flow rate (kg/s)	MPC	Model predictive control
$Q_i$	Actual heat load (kW)	MSE	Mean squared error
$\widehat{Q}_i$	Predicted heat load (kW)	RBF	Radial basis function
R	Reaction rate	RES	Renewable energy source
$T_s$	Solid material temperature (K)	STES	Seasonal thermochemical energy storage
$T_g$	Fluid temperature (K)	SVR	Support vector regression
$S_h$	Heat source (W/m)	TCES	Thermochemical energy storage
$w_{ji}$	Hidden layer weights	<i>Subscripts</i>	
x	Inputs of machine learning models	s	Solid
<i>Greek letters</i>		g	Fluid
$\rho$	Density ( $kg/m^3$ )	i	Internal
$\epsilon$	Desired error range for all data points	j	Time step
$\lambda$	Thermal conductivity (W/m.K)		

## 1. Introduction and literature review

The transition towards sustainable energy systems is essential to mitigate climate change and reduce dependence on fossil fuels. In regions with cold climates, such as the UK, a significant portion of thermal energy consumption in buildings is dedicated to space heating and domestic hot water [1], with approximately 90% supplied by gas or oil-burning boilers [2]. This reliance contributes significantly to greenhouse gas emissions and substantial waste heat production [3]. Achieving the UK's carbon neutrality target by 2050 requires efficient heating solutions that minimize waste heat and incorporate renewable energy sources, supported by advanced storage technologies.

Efficient heating solutions, such as district heating (DH) systems, are crucial for the transition towards sustainable energy systems. DH systems provide centralized heat to residential and commercial buildings by generating heat at a central plant and distributing it through insulated pipes, ensuring efficiency and reliability. Additionally, DH systems can utilize various energy sources including renewable energy, waste heat from industrial processes, and more efficient combined heat and power (CHP) systems. However, a key challenge for DH systems is the seasonal mismatch between heat supply and demand, leading to operational inefficiencies and an increased reliance on fossil fuels to meet peak demand [4].

Seasonal thermal energy storage systems can effectively address the seasonal imbalance between heat supply and demand by storing excess thermal energy during low-demand periods, such as summer, and releasing it during high-demand periods in winter. Among seasonal thermal energy storage technologies, thermochemical energy storage (TCES) stands out due to its high energy density, long-term storage capability, and ability to discharge heat at high temperatures. TCES systems use reversible chemical reactions to store and release energy, making them ideal for integration with DH systems [5–7].

Installing thermal storage systems in DHs reduces reliance on peak-time energy sources, thus increasing the efficiency of primary energy consumption through thermal energy shifting. When selecting the appropriate type of thermal energy storage system, the discharging temperature levels should be considered to be compatible with DH

systems. TCES is particularly advantageous due to its operational flexibility, allowing it to adapt to various temperature discharging scenarios [4].

To maximize the efficiency of TCES systems within DH networks, it is essential to develop and optimize effective control strategies, as these strategies ensure that energy is stored and released at the most advantageous times. A promising approach is model predictive control (MPC), an advanced technique that forecasts future system responses and makes optimal decisions based on multiple objectives and constraints. By utilizing MPC, the charging and discharging cycles of TCES systems can be dynamically managed, ensuring efficient energy use throughout the year.

However, implementing MPC for TCES in DH systems presents several challenges, such as accurately predicting heat demand, managing the variability of energy sources, and ensuring scalability and robustness. Machine learning models, particularly those capable of multi-step forecasting, provide a solution for precise heat load prediction, which is crucial for effective MPC operation. By integrating machine learning with MPC, the performance of TCES systems can be enhanced, thereby improving the overall efficiency of DH networks.

This research aims to develop an MPC control strategy for a seasonal thermochemical energy storage system (STES) within a district heating network. The proposed approach integrates machine learning models for accurate heat load prediction and evaluates system performance under various supply capacity scenarios. Using a case study in Nottingham, UK, this research seeks to demonstrate the feasibility and benefits of integrating STES with advanced control strategies in real-world DH applications.

To further explore the potential and optimize the implementation of STES within district heating networks, the following subsections investigate the current advancements in seasonal thermal energy storage technologies, the principles and benefits of thermochemical storage systems, the application of MPC strategies, and the integration of machine learning predictive models to enhance system performance and efficiency.

### 1.1. Advancements in seasonal thermal energy storage

Recent advancements in seasonal thermal energy storage systems showcase a variety of innovative approaches aimed at improving energy efficiency and reducing emissions. For instance, Mahon et al. [3] developed a seasonal thermal energy storage system along with an advanced model-based control. Their study evaluated the feasibility of the proposed system in terms of payback time, charging expense, and installation cost, confirming its advantages in energy and CO<sub>2</sub> reduction (4.3% of the residential CO<sub>2</sub> output). In a different approach, Alkhalidi et al. [8] investigated a seasonal thermal energy storage charged during the summer using solar collectors. Given the seasonal nature of solar radiation, the stored heating energy was intended for use in winter, and the results showed that the proposed seasonal thermal energy storage systems could meet up to 84% of the heating demand.

Li et al. [9] proposed a dual-mode thermochemical sorption energy storage method for seasonal solar thermal energy storage with minimal heat losses. During the summer charging phase, solar energy is stored via a thermochemical decomposition process, allowing it to be kept at ambient temperature for months. In winter, the stored energy is released through a thermochemical synthesis process. This method achieved a coefficient of performance (COP) of 0.6 and an energy density exceeding 1000 kJ/kg of salt. In a different approach, Yang et al. [10] conducted a techno-economic-environmental analysis of seasonal thermal energy storage with solar heating for residential use in China. They considered the local context, performance, and feasibility of the system. Their findings highlighted that STES reduced CO<sub>2</sub> emissions by 52–72% compared to conventional systems, although the heating costs were higher. Furthermore, Benzaama et al. [11] developed a seasonal thermal energy storage system with an earth-air heat exchanger to improve thermal energy efficiency. A case study conducted on a test cell in Oran, Algeria, demonstrated energy savings of 233 kWh and a reduction in CO<sub>2</sub> emissions of 21 t during the heating period.

The ongoing research highlights the potential of seasonal thermal energy storage systems to address seasonal energy supply and demand imbalances, offering energy savings and contributing to emission reductions. Integrating these storage systems with district heating networks can further enhance their efficiency and sustainability.

### 1.2. Developments in thermochemical energy storage (TCES) system

Building on the advancements in seasonal thermal energy storage, thermochemical energy storage (TCES) systems offer a promising approach for long-term thermal energy storage. TCES systems utilize reversible chemical reactions to store energy in a chemical form, which can later be converted back to thermal energy as needed. These systems are particularly notable for their ability to offer stability across a range of temperatures [12,13]. The potential for achieving high energy density and operating at elevated temperatures has driven increased interest in TCES systems [14].

Recent research has explored various applications of TCES, particularly in solar energy, showing potential for enhancing energy efficiency. Wong [15] examined TCES for concentrated solar power (CSP) plants, utilizing thermochemical cycles with reversible REDOX reactions of oxides like cobalt and manganese. The system stores energy by reducing oxides with hot air during daylight and releases it through re-oxidation at night, enabling an 8-h charge-discharge cycle, achieving storage costs around \$40/kWh. Similarly, Singh et al. [16] focused on a cobalt/cobaltous oxide (Co<sub>3</sub>O<sub>4</sub>/CoO) redox cycle using a cordierite honeycomb structure, functioning as both a heat storage medium and heat exchanger. A numerical model accurately predicted the charging and discharging processes, validated by experiments from a 74 kWh prototype reactor at the Solar Tower Jülich facility in Germany.

Expanding on solar thermal storage, Li et al. [17] investigated TCES for district heating in China, utilizing the MgO/Mg(OH)<sub>2</sub> system. Their study showed stored thermochemical energy could meet 94.6% of

heating demand during the discharging stage, with a required solar collector area two-thirds smaller than that for a water storage tank of similar volume. Chen et al. [18] developed an ammonia-based solar TCES system to produce supercritical steam for electricity generation, heating steam from approximately 350 °C to 650 °C at 26 MPa. Han et al. [19] highlighted materials used in TCES for CSP plants, noting high energy storage density and compatibility of metal oxides with CSP temperatures. Cobalt oxides, despite their high energy density, face cost and toxicity challenges, while manganese oxides are stable and inexpensive but have lower energy density, and copper oxide struggles with melting issues despite its high energy density. These studies demonstrate the versatility and efficiency of TCES systems in solar energy applications.

In addition to solar energy, TCES systems have shown considerable promise in utilizing industrial waste heat for energy storage and recovery [20]. Nagamani et al. [21] evaluated a mobile TCES system using industrial waste heat. Their analytical model assessed energy efficiency, round-trip efficiency, COP, and exergy performance, finding an average round-trip efficiency of 53%, a maximum COP of 1.74, and an exergy efficiency of 46.7%. The MTES truck demonstrated potential for sustainable cooling in district energy networks. Böhm and Lindorfer [22] assessed thermochemical materials for seasonal heat storage in district heating, identifying hydration-based materials combined with industrial waste heat as the most cost-effective, with production costs around 100 €/MWh.

Li et al. [23] proposed a solid-gas thermochemical sorption heat transformer for integrated energy storage, cooling, heating supply, and waste heat recovery. This system offers 10 times higher energy density than conventional methods, making it suitable for large-scale industrial processes. Li et al. [24] developed a similar system that upgrades low-grade waste heat from 87 to 171 °C using reversible chemical reactions with MnCl<sub>2</sub>-CaCl<sub>2</sub>-NH<sub>3</sub>, allowing flexible temperature adjustments. Mastrorardo et al. [25] developed hybrid materials using magnesium hydroxide with expanded graphite and carbon nanotubes for waste heat storage, improving reaction rates and efficiency.

Gao et al. [26,27] explored systems to utilize engine exhaust waste heat for truck refrigeration. They developed a compression-assisted thermochemical sorption system with a COP of 1.65 at low load and 1.48 on average. Another system combined vapor-compression with thermochemical resorption, achieving 2.2 kW cooling at -15 °C and doubling efficiency. Yan et al. [28] developed a thermochemical adsorption heat storage system using MnCl<sub>2</sub>-NH<sub>3</sub> with expanded graphite, achieving a heat storage density of 3211.56 kJ/kg and an efficiency of 0.939, proving effective for solar thermal energy harvesting and industrial waste heat recovery. These studies demonstrate the versatility and efficiency of TCES systems in waste heat applications.

Innovative control strategies have been developed to enhance efficiency and cost-effectiveness of TCES. Weber et al. [29] developed an MPC system for cost-efficient building climate control using thermochemical seasonal energy storage. The system stores summer surplus electricity for winter heating, reducing operating costs by 18% in realistic scenarios and up to 80% with fluctuating electricity prices, without needing long-term weather forecasts.

Moreover, practical evaluations of TCES systems have demonstrated their robust performance and high storage capacity. Tescari et al. [30] evaluated a pilot-scale thermochemical storage system for a solar power plant using 88 kg of cobalt oxide on cordierite honeycomb supports. Over 22 charge-discharge cycles, the system showed no degradation and achieved a performance factor of 0.84. It provided nearly double the storage capacity (47.0 kWh) compared to a sensible-only unit (25.3 kWh).

Coupling energy storage systems with decarbonization targets is essential [31]. TCES systems are notable for their high energy density and ability to operate at elevated temperatures, which can provide significant advantages in specific applications [32]. Their ability to provide flexibility, long-term storage [33], and adaptable discharge

temperatures offers potential for district heating networks. By capturing and utilizing surplus heat from various sources and storing energy over extended periods, TCES ensures a steady supply even during peak demand periods. Integrating TCES can also enhance the efficiency of CHP systems within district heating by reducing the need for frequent adjustments and optimizing overall energy use [34–36]. Utilizing TCES allows district heating networks to enhance sustainability, efficiency, and cost-effectiveness.

### 1.3. Model predictive control (MPC) for optimizing seasonal thermal energy storage

Building on the discussion of seasonal thermal energy storage systems as a promising solution to address the seasonal mismatch between heating energy supply and demand, it is crucial to focus on the proper design and effective control strategies for these systems. Properly sizing the storage system [8] and implementing an effective control strategy are essential for maximizing performance, minimizing waste heat, and reducing CO<sub>2</sub> emissions. This section explores into the use of MPC to optimize the operation of seasonal thermal energy storage systems.

Li et al. [37] highlighted the importance of control strategies in enhancing the performance of a solar heating system coupled with seasonal thermal storage, showing that optimized control significantly improved heat collection and exergy efficiency. MPC is one such strategy that optimizes operation by predicting future system states and adjusting the storage system accordingly. In the case of thermal storage, employing MPC allows the system to activate storage during low-demand periods and release energy during high-demand periods, leading to overall economic gains [38]. Building on this concept, Jonin et al. [39] demonstrated the effectiveness of an MPC scheme for a large-scale seasonal thermal energy storage tank connected to a solar panel, which efficiently managed space heating and domestic hot water demands. They incorporated seasonal features into the MPC, optimizing both system exergy and storage tank size while ensuring user demand was met.

Expanding on the use of MPC, Milewski et al. [40] proposed an objective function based on techno-economic assumptions to optimize the system's operation. They developed mathematical models for the main components and validated the approach with simulations, demonstrating its suitability for MPC in managing seasonal thermal energy storage effectively. Similarly, Rostampour et al. [41] developed a stochastic MPC framework for smart thermal grids using aquifer thermal energy storage systems, addressing thermal energy imbalances and uncertainties, and providing a computationally tractable solution for optimizing building climate comfort.

Saloux et al. [42] developed an MPC strategy for a district heating system, which uses solar thermal collectors and a borehole field for seasonal energy storage. By optimizing circulation pump speed, the strategy minimizes primary energy consumption, achieving a 47% reduction in annual pump electricity use, a 38% cost savings, and a 32% decrease in emissions. Lago et al. [43] developed control algorithms for seasonal thermal energy storage systems to trade on wholesale electricity markets, using MPC for day-ahead markets and reinforcement learning for real-time markets. Their study showed that these strategies maximize operational profit, mitigate renewable energy uncertainty, and help reduce grid imbalances.

MPC has proven effective for optimizing seasonal thermal energy storage systems. Studies demonstrate that MPC improves energy efficiency, economic gains, and CO<sub>2</sub> emission reductions. By predicting future system states and adjusting storage operations, MPC can enhance the performance of district heating systems.

### 1.4. Machine learning predictive model for heat load forecasting

Accurately predicting heat loads is crucial for the effective formulation of model predictive frameworks. Reliable heat load prediction

enables the optimization of MPC in seasonal energy storage, allowing for efficient redistribution of heat supply, minimizing losses, and enhancing overall energy efficiency. Traditionally, heat load forecasting methods have relied on physics-based models, which use fundamental physical principles and empirical data to predict heat demand. These models are based on theories of heat transfer and other physical processes. In contrast, data-driven models offer significant advantages by utilizing large datasets to identify complex patterns and relationships that may not be explicitly captured by physics-based approaches.

Data-driven methods such as machine learning can identify latent correlations between heat loads. These methods derive parameters directly from operational data, enabling more precise and adaptable control strategies within MPC frameworks. Machine learning, a subset of artificial intelligence, enables numerical models to learn from data, reducing the need for complex rule-based programming. However, domain expertise remains important for selecting appropriate models and interpreting their results effectively. By utilizing historical data and real-time inputs, machine learning models can provide accurate and reliable heat load forecasts, which are critical for the effective implementation of MPC strategies in district heating systems. This integration of machine learning enhances the predictive capabilities of MPC, ensuring efficient and optimized energy management.

Numerous studies have explored and assessed the suitability of different machine learning algorithms for forecasting heat loads in district heating systems. Commonly employed algorithms include linear regression [44], seasonal autoregressive integrated moving average [45], support vector machine [46], extreme gradient boosting [47], and regression tree [46]. These machine learning models have proven to be reliable tools for predicting building heating loads, demonstrating their potential to significantly enhance the efficiency and effectiveness of MPC in managing district heating systems.

For example, Grosswindhager et al. [48] used a seasonal autoregressive integrated moving average model to predict heat loads in district heating networks, achieving high accuracy and suitability for online short-term forecasting. Wang et al. [49] developed a dynamic model combining wavelet analysis and neural networks to predict heat demand using outdoor temperature and heating system characteristics, demonstrating superior accuracy and tracking performance compared to other methods for short-term thermal load forecasts.

Xue et al. [47] proposed a machine learning-based framework for multi-step ahead heat load forecasting in district heating systems, using support vector regression, deep neural networks, and XGBoost. They demonstrated that the recursive strategy with the XGBoost model achieved the most accurate and stable predictions, with a CVRMSE of 10.52%. Idowu et al. [46] used district heating data from 10 buildings to forecast thermal loads, finding that support vector machine had the lowest normalized root mean square error (NRMSE) of 0.07 for a 24-h forecast horizon, outperforming regression tree, feed-forward neural network, and multiple linear regression models. Common input variables for these models included time variables, meteorological parameters, and historical heat load data. These findings highlight the importance of selecting suitable machine learning methods and input variables to improve prediction accuracy and reliability in district heating systems.

As mentioned earlier, machine learning-based predictive models offer a more intuitive and convenient tool for district heating heat load prediction compared to traditional physics-based models. However, these approaches face limitations, particularly as many studies often focus on short-term predictions (e.g., 1-h intervals). This short-term focus can limit their effectiveness for long-term energy management and planning in district heating systems.

In the context of seasonal thermal energy storage operations, it is crucial for the controller to anticipate the upcoming seasonal heat load profile to effectively strategize heat supply and storage planning. To meet this requirement, a recursive demand prediction based on a multi-step forecasting approach is employed. At each time step, the algorithm

predicts the next time step ( $t + 1$ ) and uses this prediction as an input for the following step ( $t + 2, t + 3, \dots, t + n$ ). This process continues using the same machine learning model until the heat load profiles across the entire prediction horizon are generated.

### 1.5. Novelty, aims and objectives

Despite the promising potential of seasonal thermal energy storage systems and the advantages of MPC in optimizing energy use, gaps remain in the literature. Current research primarily focuses on short-term and medium-term storage solutions, with less emphasis on the integration and long-term performance of STES within district heating systems. While various machine learning algorithms have proven effective in predicting heat loads, their application in multi-step forecasting for long-term STES operations is limited. Additionally, existing studies often overlook the practical implementation challenges of these integrated systems, particularly under varying demand scenarios.

Moreover, while the development of MPC strategies for seasonal thermal energy storage has been explored, the combination of MPC with machine learning for dynamic energy management in district heating systems remains under-researched, particularly in the context of seasonal thermal energy storage. Further research is required to compare the effectiveness of various control strategies (e.g., rule-based control, MPC) in district heating contexts to identify the most efficient and practical approaches. Ensuring the scalability and robustness of MPC strategies when integrated with machine learning for large-scale district heating networks requires further exploration. A comprehensive approach is needed that incorporates predictive models to optimize the charging and discharging cycles of thermochemical energy storage systems within district heating networks. This approach should address the seasonal mismatch between supply and demand, minimize waste heat, and enhance overall system efficiency.

This study aims to provide insights into the feasibility and potential of integrating seasonal thermal energy storage with an intelligent MPC control strategy. A numerical thermochemical storage system is incorporated within the MPC framework to illustrate how MPC makes decisions on energy charging and discharging, using predictive models enhanced by machine learning techniques for DH systems. The MPC strategy seeks to minimize thermal energy waste by storing surplus energy in the seasonal thermal energy storage system and utilizing it in subsequent seasons. To evaluate the practicality and effectiveness of the integrated system, scenario analyses with different rates of supply reduction will be conducted, examining supply efficiency under varying conditions.

Our contributions in this study are as follows:

- We propose a multimode control method for the district heating system, which addresses different building patterns within the same substation. Unlike traditional multimode approaches in DH demand forecasting that rely on multiple physical-based models, our method creates a single prediction model. This significantly reduces computational costs and meets the real-time demands of control processes in practical applications.
- The proposed approach includes a multi-step ahead prediction model specifically designed for the MPC strategy. This model compares the effectiveness of three machine learning algorithms: support vector regression (SVR), long short-term memory network (LSTM), and regression tree. The effectiveness of this method is demonstrated using a case study of an actual district heating system in Nottingham, UK.
- We introduce a seasonal storage MPC method to store surplus heat generated in the summer for use during the winter. The primary objective of this MPC strategy is to minimize the annual waste heat, thereby enhancing the overall efficiency and sustainability of the district heating system.
- We will compare the proposed MPC strategy with a traditional rule-based control approach to evaluate the performance improvements. This comparative analysis will highlight the advantages and potential of MPC

in district heating applications.

## 2. Method

This section outlines the methodology used to create an MPC system for controlling STES. Initially, machine learning models are developed for demand prediction, followed by validation using real-world DH demand profiles. The thermochemical storage model is also presented, along with its integration into the MPC strategy. The development of the MPC model involved numerical modeling and simulations conducted on the MATLAB platform.

### 2.1. Machine learning for district heating demand forecasting

Training a machine learning model generally involves two segments: training data and testing data, both derived from the same dataset. The training set, which constitutes a large portion of the dataset, is used to train the model, while the testing set is used to evaluate the model's performance. According to the study [47], it is suggested to allocate 80% of the data samples for training and reserve 20% for testing. Following this approach, we partitioned our dataset into 80% for training and 20% for testing.

Three main types of influential parameters in DH heat load prediction, according to [47], are weather conditions, time-related variables, and DH operational characteristics. Among meteorological parameters, outdoor temperature has been demonstrated as a primary influential

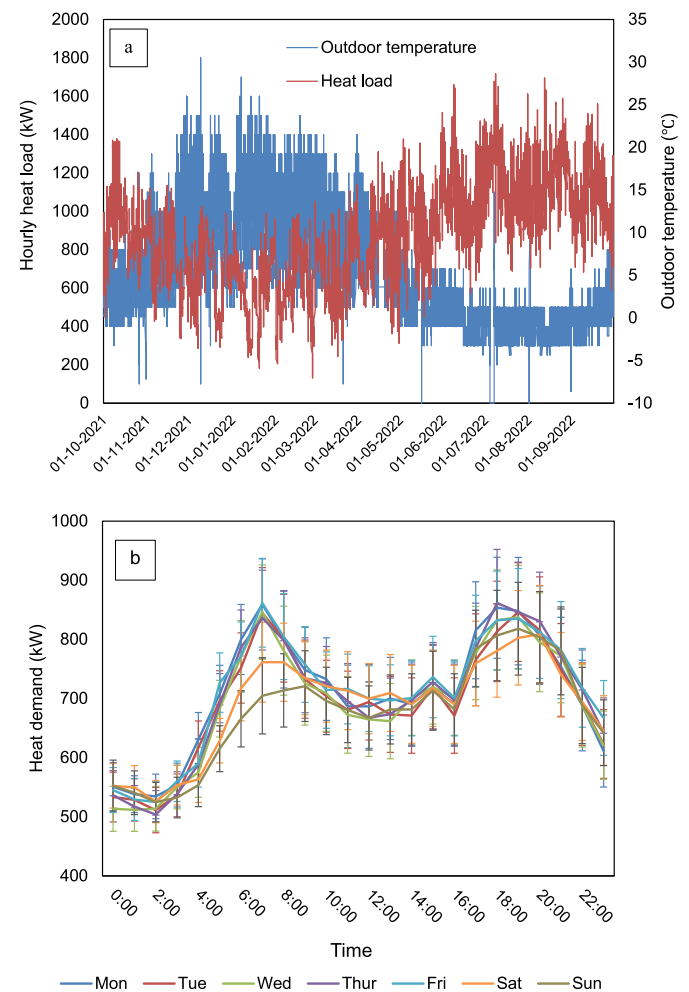


**Fig. 1.** (a) Time series representation of heat load and outdoor temperature over the same period, and (b) average hourly heat demand in a day with standard deviation for the entire year.

factor in predicting DH heat load, as shown in the study [48]. Fig. 1a illustrates that heat demand is primarily influenced by ambient temperature. Fig. 1b shows the average hourly heat demand over a day, along with the standard deviation for the entire year. The standard deviation (represented by error bars in Fig. 1b) is calculated based on squared differences between each hourly demand and the average hourly demand.

Daily demand often varies depending on the hours of the day (Fig. 1b). Consequently, we chose 24 h in a day as influential variables in our demand forecasting model. Historical heat load data also contains valuable information, including building thermal inertia, time-based regulation strategies, and building types. In this study, we utilized outdoor temperature and heat load measured over the previous 12 h, following the approach outlined in [47], to ensure faster computational time.

Following the selection of influential parameters for our machine learning models, it was essential to transform categorical features into numerical ones. We employed the one-hot encoding method to quantify categorical variables, as per the guidelines in reference [50]. Specifically, we used one-hot encoding to convert the numbers 1 through 24, representing hours, into 24 binary variables. For the hour corresponding to the current time step, the variable is set to 1, while the remaining 23 variables are set to 0. This data preparation resulted in 24 binary variables for the hours, 12 features of historical heat load, and one outdoor temperature variable, amounting to a total of 37 features used for heat load prediction.

When using our machine learning model for forecasting long-term heat demand, we applied a recursive strategy as outlined in reference [47]. At each time step, the predicted one-step future demand is fed into the next prediction as an influential variable. This process continues iteratively until predictions are made for the entire prediction horizon, which, in our study, spans one year (Fig. 2).

## 2.2. Machine learning models

Machine learning methods entail learning a mapping from an input dataset to an output dataset, based on a labelled set of input-output pairs. Commonly employed machine learning methods include neural network-based algorithms, support vector regression (SVR), and regression trees, as highlighted in studies [51,52]. The subsequent section outlines the technical details for each of these methods. In this study, the machine learning model is applied to both the MPC and a reference rule-based control strategy for demand prediction.

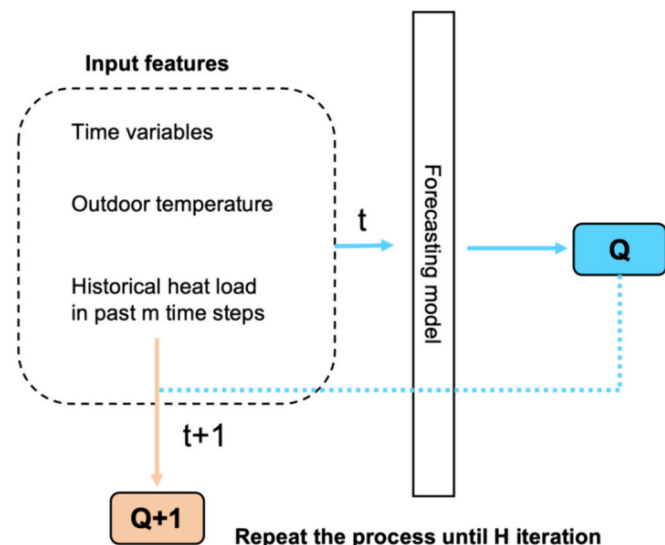


Fig. 2. H-step ahead heat load forecasting using the recursive strategy [47].

### 2.2.1. Support vector regression (SVR)

Support vector regression (SVR) is based on principles similar to linear regression but extends them by using kernel functions to handle non-linear relationships. This makes SVR well-suited for complex non-linear optimization problems, which are common in demand forecasting. SVR maps the feature space created by the training dataset to a higher-dimensional feature space using a kernel function. In this high-dimensional space, SVR identifies a hyperplane that best fits the training data. The optimal solution is found by minimizing the following convex function [53]:

$$\frac{1}{2} \|w\|^2 + C \sum_{i=1}^l \varphi_i + \varphi_i^* \quad (1)$$

With the constraints:

$$y_i - w^T \varnothing(\bar{x}_i) - b \leq \epsilon + \varphi_i \quad (2)$$

$$w^T \varnothing(\bar{x}_i) + b - y_i \leq \epsilon + \varphi_i^* \quad (3)$$

Where  $\epsilon$  represents the desired error range for all data points.  $\varphi_i$  and  $\varphi_i^*$  are slack variables.  $C$  is the penalty term used to balance data fitting and smoothness.  $\varnothing$  refers to a kernel function used for high-dimensional mapping. This formulation allows SVR to handle the non-linearities in the data effectively, making it suitable for complex demand forecasting tasks.

### 2.2.2. Regression tree

A regression tree is a tree structure designed to predict continuous output values by mapping input instances to leaves [54]. Specifically tailored for regression tasks, it constructs a binary tree using a greedy approach in a top-down recursive divide-and-conquer manner. This method divides the large training data into smaller subsets corresponding to the leaves of the regression tree. The split criterion for the regression tree is based on minimizing the prediction error. This approach is effective for capturing complex, non-linear relationships in the data, making regression trees a valuable tool for demand forecasting in district heating systems.

### 2.2.3. Long short-term memory (LSTM)

Neural network (NN) models are among the most extensively utilized machine learning models [55]. Configuring a neural network requires defining its structural components, including the number of hidden layers, hidden units, and other pertinent parameters. The predictor ( $y$ ) in a neural network model can be represented by a generic expression involving the inputs ( $x$ ), as illustrated in the following equation:

$$y = f_0 \left( \sum_{j=0}^{N_h} w_j f_h \left( \sum_{i=0}^K w_{ji} x_i \right) \right) \quad (4)$$

where  $f_0$  is the output layer activation function,  $f_h$  is the hidden layer activation function,  $w_j$  is the output layer weights,  $w_{ji}$  are hidden layer weights.

The long short-term memory (LSTM) network features an enhanced structure that enables it to effectively retain crucial features from earlier time-series data. The LSTM architecture incorporates distinct gates, which progressively learn the mapping between historical input sequences and the predicted output sequence. The input gate decides how much incoming information should be stored in the memory block, while the forget gate determines which information should be omitted. The retained information is stored in the memory cell, and finally, the output gate filters this information to produce the network's output [56]. This structure allows LSTM networks to handle long-term dependencies in time-series data, making them highly effective for tasks such as demand forecasting in district heating systems.

### 2.2.4. Model evaluation and platform

After creating the models, we employed the trained machine learning models to predict heat load on the test dataset. The performance of these models was assessed using two key metrics: mean absolute error (MAE) and the coefficient of variation of root mean square error (CVRMSE). The equations for MAE and CVRMSE are as follows:

$$MAE = \frac{1}{n} \sum_{i=1}^n |Q_i - \widehat{Q}_i| \quad (5)$$

$$CVRMSE = \frac{1}{\bar{m}} \sqrt{\frac{\sum_{i=1}^n (Q_i - \widehat{Q}_i)^2}{n}} \times 100 \quad (6)$$

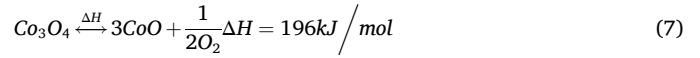
where  $Q_i$  and  $\widehat{Q}_i$  represent the actual and predicted heat loads, respectively,  $n$  is the number of observations, and  $\bar{m}$  is the mean of the measured values.

The mean absolute error (MAE) is a scale-dependent metric that can be used to compare overall performance with similar studies. It provides an average measure of the errors between predicted and actual values. The coefficient of variation of root mean square error (CVRMSE), on the other hand, accounts for the scale of the data and provides a normalized measure of the prediction error. While CVRMSE normalizes the error, it can still be influenced by outliers due to the squaring of errors. CVRMSE allows for a more consistent comparison across different datasets and conditions.

This study was conducted using Matlab R2019a [57], leveraging its Deep Learning Toolbox for the LSTM model, and utilizing the built-in functions “fitsvm” and “fitree” for SVR and regression tree implementations, respectively. Both the SVR and regression tree models required minimal or no parameter tweaking. For SVR, we selected the Gaussian function within the radial basis function (RBF) as the kernel model. Regarding the LSTM algorithms, this investigation employed a 4-layer LSTM network based on the findings in the study [46]. The network layers included a sequence input layer, an LSTM layer, a dropout layer, and a fully connected layer. Finally, for each control implementation, machine learning demand predictions were run once to extract one-year demand forecasts and next-hour demand forecasts for MPC and rule-based control, respectively.

### 2.3. Thermochemical energy storage system model

The TCES system model used for our MPC was validated with that of [16], which represents a scaled-down version of a storage unit that includes ceramic honeycombs. Within the chamber, the reactants consist



The process is detailed as follows: Initially, there is only sensible heat transfer from the high-temperature fluid to the solid material until the solid temperature reaches the reduction temperature of  $\text{Co}_3\text{O}_4$  (around 1164 K at 1 bar pressure). The chemical reaction proceeds until all  $\text{Co}_3\text{O}_4$  is converted to CoO. The CoO remains stable until the solid temperature decreases to the oxidation temperature (around 1164 K at 1 bar pressure) by flowing low-temperature fluid into the honeycomb structure. During the chemical reaction, the solid temperature tends to remain constant, forming a plateau.

The one-dimensional numerical model developed in MATLAB by Zhou et al. [59] was used and then reformulated as a state space model for the proposed MPC. The model is based on the following assumptions:

- The distribution of initial  $\text{Co}_3\text{O}_4$  is assumed to be uniform.
- Conduction is considered only in one dimension along the flow direction.
- The initial temperature of each temperature node is assumed to be the same.
- The change in oxygen concentration is neglected.
- The flow rate is considered constant from inlet to outlet.
- The diffusion effect of the reaction is not considered.

#### 2.3.1. Heat transfer modeling

The heat transfer process involves both conduction in the solid material and convective heat transfer between the fluid and solid surfaces. Thermal non-equilibrium separate energy equations are applied for each phase [59]. Fig. 3a shows the cross-section of each cell in the honeycomb reactor, while Fig. 3b illustrates the temperature node distribution in the mathematical model of the TCES. Here,  $T_f$  and  $T_s$  represent the temperature nodes of the fluid and solid, respectively. Heat transfer, either through convection or conduction, is depicted by the interaction between each pair of temperature nodes.

The equations below illustrate the thermal non-equilibrium separate energy equations for solid and air phases. They are developed and validated in the study of Zhou et al. [59].  $A_f$  is the total flow area of all channels and  $A_c$  is the total heat transfer area of all channels.  $A_s$  is the cross section area of the solid. Heat transfer, represented by Eqns. 8 and 9, includes both conduction and convection between the denoted node and neighboring nodes.

Solid:

$$\rho_{st}^j \bullet A_s \bullet dx \bullet C_{st}^j \frac{T_{si}^{j+1} - T_{si}^j}{dt} = \lambda_i \frac{T_{si}^{j+1} - 2T_{si}^{j+1} + T_{si+1}^{j+1}}{dx} + h_i^j A_c \left( \frac{T_{gi}^{j+1} + T_{gi+1}^{j+1}}{2} - T_{si}^{j+1} \right) + S_{hi}^j \bullet dx \quad (8)$$

of cordierite coated with  $\text{Co}_3\text{O}_4$ . The redox pair of  $\text{Co}_3\text{O}_4/\text{CoO}$ , governed by Eq. 7, has an equilibrium temperature of around 900 °C at atmo-

Fluid:

$$\rho_{gi}^j \bullet A_f \bullet dx \bullet C_{gi}^j \frac{T_{gi}^{j+1} - T_{gi}^j}{dt} = \dot{m}_{i-1} C_{pi-1}^j T_{gi-1}^{j+1} - \dot{m}_i C_{pi}^j T_{gi}^{j+1} - h_i^j A_c \left( \frac{T_{gi}^{j+1} + T_{gi+1}^{j+1}}{2} - T_{si}^{j+1} \right) \quad (9)$$

spheric pressure. This redox pair has a high energy density and long-term material stability [58].

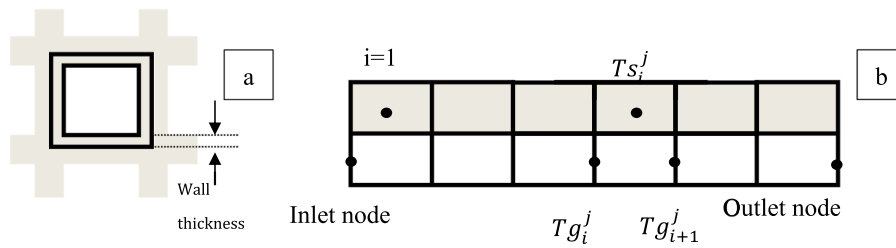


Fig. 3. (a) Cross section of each cell in the honeycomb reactor, and (b) temperature node distribution in the mathematical model of the thermochemical energy storage model.

The thermodynamic properties of fluid, which are typically temperature-dependent, are obtained from the NIST REFPROP database [60]. For solid materials, the thermodynamic properties are calculated by summing the fraction of each part of cobalt oxides ( $f$ ) and the mass fraction of cordierite ( $1 - \varphi$ ). Here,  $\varphi$  represents the thermodynamic properties of each solid material [16].

$$\varphi = \varphi \sum_i (f_i \cdot \varphi_i) + (1 - \varphi) \cdot \varphi_{\text{cordierite}} \quad (10)$$

Where  $i$  denote the respective cobalt oxide species.

The chemical heat source  $S_h$  is introduced by multiplying the reaction rate  $R$ , concentration of reactive species  $C$  and enthalpy  $\Delta H$ , in which both of reaction rate and concentration are time dependent bases on the study of [16].

$$S_{h(t)} = \Delta H \cdot R_t \cdot C_t \quad (11)$$

### 2.3.2. Model validation

The validation of the numerical model was performed by comparing the experimentally measured temperatures, as reported in the study [16], at the top and middle of the honeycomb with the model's predictions over a specific time period. This validation was conducted using the same inlet temperature and mass flow rate (Fig. 4).

The solid lines represent the experimental results from the reference study, while the dashed lines show the simulation results from the numerical model. The simulated temperatures of the solid and the fluid outlet closely match the experimental temperatures, confirming the feasibility and applicability of the numerical model in simulating the thermochemical storage system. The mean squared error (MSE) for the solid temperature and outlet temperature are 17.31 K and 19.85 K, respectively. The maximum deviation of solid temperature and outlet air temperature between the simulation and experimental results are 4.1% and 7.1% (Fig. 5).

This process explains the observed behavior by detailing the phases of heat transfer and chemical reaction within the thermochemical storage system. Initially, sensible heat transfer occurs from the high-

temperature air to the solid until the solid reaches the reduction temperature of  $\text{Co}_3\text{O}_4$  (1164 K at 1 bar). The concentration of reactive species changes as the reaction progresses, continuing until all  $\text{Co}_3\text{O}_4$  converts to  $\text{CoO}$ .  $\text{CoO}$  remains stable until the temperature decreases to the oxidation temperature (1164 K at 1 bar) during the energy discharge phase, facilitated by low-temperature air flowing into the honeycomb structure.

### 2.4. Model predictive control (MPC) formulation

MPC is an advanced control method that makes real-time decisions for the system by predicting future system responses. MPC allows users to input multiple objectives into its formulation and then make decisions aimed at minimizing the cost of these objective functions while ensuring adherence to system operating constraints. MPC typically relies on time-dependent models to predict the system's behavior under various future control strategies. It selects an optimal control trajectory using complex solution-searching methods. In practice, the control center only applies the first step of the optimal control strategy and discards the rest. At each time step, MPC repeats the optimization process and applies the first control signal, ensuring continuous adjustment and optimization of the system's performance.

In this study, MPC is used to make decisions regarding the heat charging and discharging of the seasonal thermochemical energy storage system (STES) system, based on the forecasted annual demand illustrated in Section 2.2. Given that MPC can become computationally intensive with a large prediction horizon, the hourly resolution was only set for the first day. For the remaining periods, three different time steps were used to manage computational costs. In the proposed MPC, 1233 time intervals were applied using four different time steps [43] (Fig. 6).

#### 2.4.1. Storage capacity identification

In MATLAB, an MPC strategy was formulated to manage the heat charging and discharging of the STES system. A decision variable  $u$  represents the heat fed into the STES system during the current time

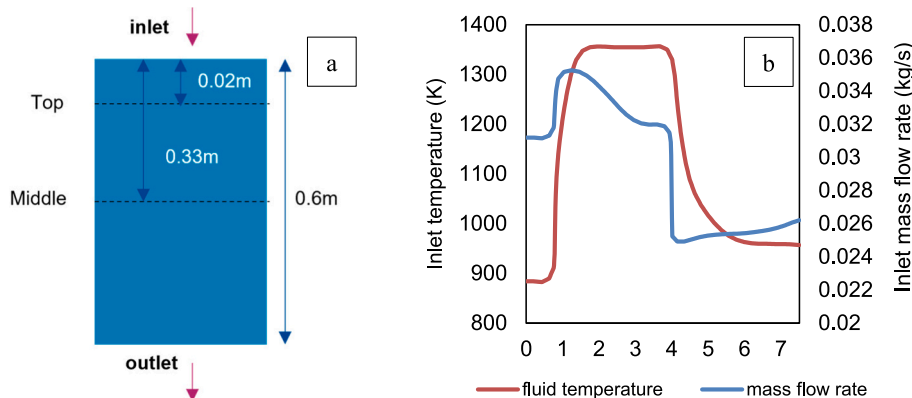


Fig. 4. (a) Schematic of the storage reactor, and (b) inlet temperature and mass flow rate in the experiment.

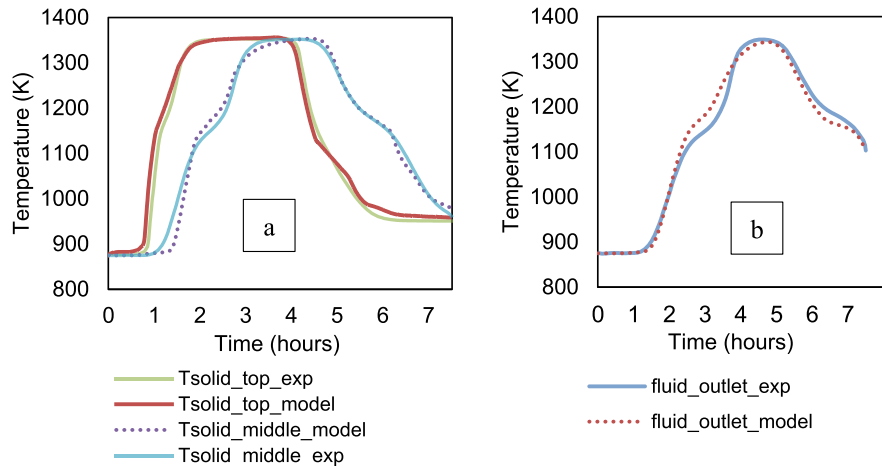


Fig. 5. Validation of the results of (a) solid temperature and (b) outlet fluid temperature.

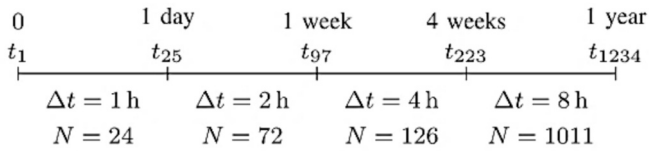


Fig. 6. Prediction horizon [43].

step. The numerical form of charge and discharge is as follows:

$$storage(k + 1) = storage(k) + u(k) \quad (12)$$

where:  $k$  represents the current time step and  $storage(k)$  denotes the amount of heat stored in the STES system at that step. The objective of the proposed MPC is minimize the total yearly waste heat:

$$objective = objective + bound(k)' \times bound(k) \quad (13)$$

Here  $bound(k)$  means the tolerance for the mismatch between heat supply and demand at the current time step. The storage capacity of the STES system and the predicted demand and supply data were constrained as follows:

$$constraints = [0 \leq storage(k + 1) \leq limited\ amount] \quad (14)$$

$$constraints = [constraints, mismatch(k) - bound(k) \leq u(k) < mismatch(k) + bound(k)] \quad (15)$$

The MPC was formulated using the Yalmip optimisation toolbox [61] and solved with the Gurobi solver [62]:

$$optimize([constraints, storage(1) = current\ storage, objective]) \quad (16)$$

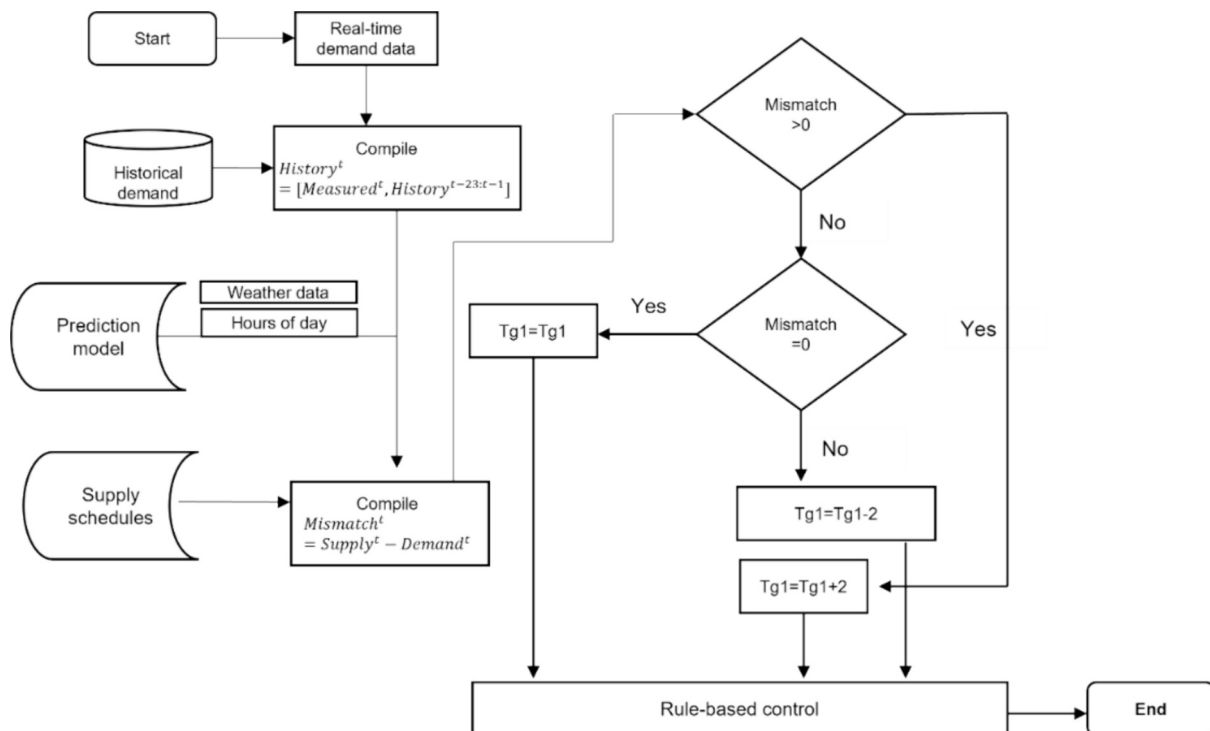


Fig. 7. Reference rule-based control.

Our system was developed with the aim of peak shaving the heating load, enabling collaborative operation with district heating (DH) during the winter. For scenario analysis, we considered storage capacities of up to 1000MWh [63], to evaluate how the system performs with different storage sizes. Additionally, we explored scenarios with various supply conditions to understand the performance and adaptability of the MPC strategy. This approach helps identify the thresholds at which the system can no longer maintain optimal performance, highlighting the limits of the current setup. Understanding these limits is crucial for planning and improving the future resilience and capacity of the system.

#### 2.4.2. Comparison of rule-based control and model predictive control (MPC)

The finalized MPC results will be compared with a rule-based control strategy (Fig. 7), which relies on a machine learning one-step ahead demand prediction [64]. In this rule-based approach, the inlet temperature is adjusted based on the mismatch between supply and demand at the start of the next hour. First, the machine learning demand prediction runs once at every control interval. The predicted demand is then compared with the scheduled supply to determine the appropriate inlet temperature for the TCES. If there is a mismatch between the predicted demand and the supply, the inlet temperature is adjusted to balance the system.

The MPC optimization problem, including the thermochemical storage model, is formulated as a mixed-integer linear program with both continuous and logic variables. The logic variables are used to model the chemical reactions within the TCES. A receding horizon approach is employed to enhance the robustness of MPC control by minimizing forecast errors over time. We reformulated the thermochemical storage model into state-space forms and increased the storage capacity to 800 MWh by maximizing the number of TCES units installed in the system, while adhering to temperature constraints. The assumptions made in the model include zero transmission loss in the DH network and the exclusion of thermal behaviors of other components such as pumping and piping systems. For simplicity, the prediction models only consider sensible gains beyond the initial 24-h prediction horizon.

Therefore, the primary objective of our MPC strategy is to minimize the mismatch between supply and demand. MPC is more robust than conventional controllers such as on/off control, PID control, and fuzzy logic control [65] when dealing with multiple conflicting objectives in an optimization problem. To incorporate thermal reactions in the model, we relaxed the integer control variables by converting them into binary variables [66]. At each time step, the reaction state (i.e., no reaction, oxidation, reduction) is represented by a distinct binary variable. A constraint ensures that the sum of the binary variables is 1, guaranteeing that only one reaction mode is active at any given time. This can be expressed as:

$$v = \sum_i^{n_v} v^i b_i \quad (17)$$

$$1 = \sum_i^{n_v} b_i \quad (18)$$

The MPC formulation is:

$$\min_{T1(t), b(t)} \int_{t_i}^{t_i+1233} (abs(supply(t) - demand(t) - store(t))) dt \quad (19)$$

subject to:

$$T_{min} < T\{t+1\} < T_{max} \quad (20)$$

$$store(t) = m \bullet C_p \bullet (T1\{t\} - T\{t\}_{outlet}) \quad (21)$$

for  $t = 1 : 24$

$$T\{t+1\} = A_1 \bullet T\{t\} + B_1 \bullet T1\{t\} + C_1 \bullet heat\{t\} \quad (22)$$

$$N\{t+1\} = N\{t\} \bullet (1 - R\{t\}) \quad (23)$$

$$heat\{t\} = H \bullet R\{t\} \bullet N\{t\} \quad (24)$$

for  $t = 25 : 96$

$$T\{t+1\} = A_2 \bullet T\{t\} + B_2 \bullet T1\{t\} \quad (25)$$

for  $t = 97 : 222$

$$T\{t+1\} = A_3 \bullet T\{t\} + B_3 \bullet T1\{t\} \quad (26)$$

for  $t = 223 : 1233$

$$T\{t+1\} = A_4 \bullet T\{t\} + B_4 \bullet T1\{t\} \quad (27)$$

In this formulation, A, B, C are the system matrices for the numerical model of the storage system.  $R\{t\}$  is the reaction rate, which is determined by the binary variables  $b(t)$  at each time step for each temperature node.  $T\{t\}$  represents the temperature nodes of the system, encompassing both fluid and solid temperature nodes.  $T1\{t\}$  is the continuous variable in the system, representing the inlet temperature as determined by the MPC. At each control step, a machine learning prediction is performed once to forecast the demand for the entire year. This predicted demand is then used to inform the MPC strategy, ensuring that the thermal storage system operates efficiently throughout the year.

### 3. Case study

The Nottingham district heating network, one of the largest and oldest in the United Kingdom, exemplifies how cities can utilize waste-to-energy solutions for heating. Fig. 8a provides an overview of the heat generation and distribution process. The system employs an energy-from-waste (EfW) facility to incinerate municipal waste collected from households and businesses. The heat generated from burning the waste produces steam, which is then transferred through heat exchangers to convert it into hot water within the heat station. This hot water circulates through the network, passing through substations before delivering heat to both commercial and residential buildings.

Substations are strategically located throughout the network to distribute heat energy to desired areas. Phase 1, situated in the St Ann's region of Nottingham, is the selected area for this study and encompasses 10 different streets, including both commercial and residential buildings. Data from one year (October 2021 to October 2022) with one-hour intervals is shown in Fig. 9, highlighting that summer heat demand is significantly lower than winter heat demand. The yearly total heat demand for Phase 1 was 5,509,300 kWh, with a daily average of 15,052 kWh.

The supply temperatures of the DH system generally hover around 83 °C, measured on the consumer's secondary side. The primary supply temperature varies throughout the year depending on the load, with summer temperatures around 85 °C/75 °C (supply/return) and winter temperatures around 110 °C/70 °C. The pumping station in the DH system sets a pressure drop to control the water flow rate, meeting varying demands throughout the day and year. The supply pressure is adjusted based on the time of day and outdoor temperature, with the highest pressure drops typically occurring during morning peak demand periods when outdoor temperatures are lowest.

The relationship between heat demand and outdoor temperatures, as shown in Fig. 1a, indicates that heat demand decreases when outdoor temperatures are high and increases when outdoor temperatures are low. For the summer months (June–September), the average temperature is 16.2 °C, with an average heat load of 422 kWh per hour. In contrast, during the winter months (December–February), the average temperature drops to 3.9 °C, and the average heat load rises to 1008



Fig. 8. (a) Heat generation and distribution across the Nottingham district heating network, and (b) pipeline of the district heating network in Phase 1 region.

kWh per hour.

To ensure that customer heat demand was satisfied at any given time, four-time bands and seven temperature intervals were applied, as shown in Table 1. The supply pressure adjusts according to a pre-determined heuristic table based on the hours of the day and outdoor temperature [67]. For example, during peak demand times and the lowest ambient temperatures of the day (5:00–9:00), the supply pressure is set to its highest level. However, this control strategy often resulted in excessive heat dissipation due to frequent mismatches between supply and demand.

We propose to apply the TCES system in our DH case study as a model for efficient heat supply and storage. This TCES system will operate alternately in storage mode or discharging mode to ensure an

uninterrupted heat supply. During the charging process, the energy storage material will undergo conversion with the assistance of thermal energy. When there is a need to release thermal energy, the reactants will generate heat through a chemical reaction [68]. The medium will flow into the reactor, where it will exchange heat with the solid material, facilitating the continuous exchange of sensible and chemical heat. During periods of excess heat generation from the power plant, the waste heat will be used to regenerate the thermochemical storage (heat storage process). At peak load demand during the space heating season, the thermochemical store will release stored heat (heat discharge process) to meet increased heat loads, thereby optimizing energy management within the DH network.

Energy charge from thermochemical storage systems can serve as an



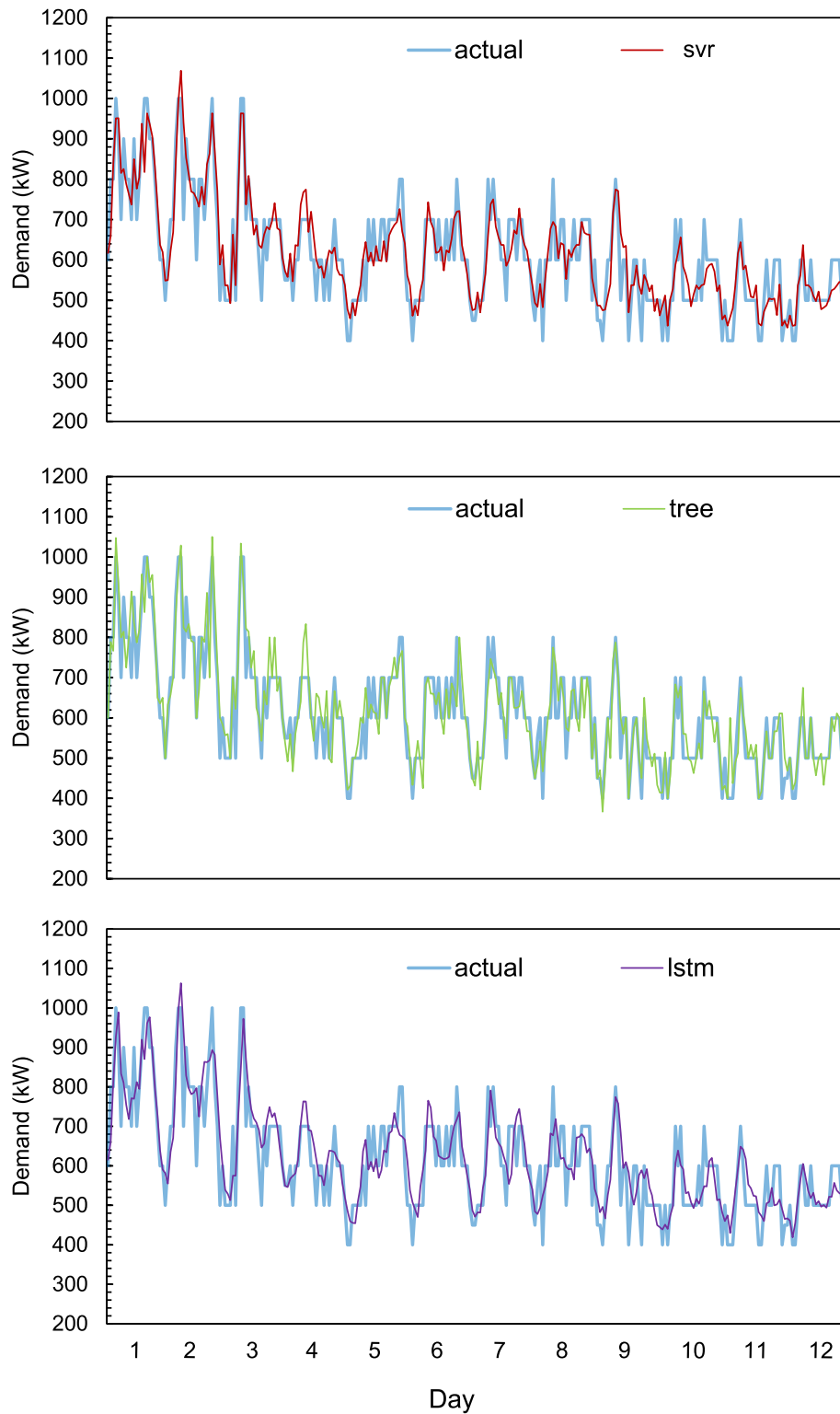


Fig. 11. Demand prediction results of different techniques.

**Table 2**  
Prediction performance of three machine learning models.

	SVR	Regression tree	LSTM
MAE (kW)	43.98	30.29	45.28
CVRMSE (%)	10.46	9.07	11.09

our study, the input variables and the response variable demonstrate a robust linear relationship, contributing to the SVR model's comparable accuracy with other machine learning techniques. Additionally, the regression tree method achieved notably high accuracy. Regression trees are typically well-suited for discrete data types with limited datasets, and the high accuracy observed in this study can be attributed to the strong correlation between the chosen input variables and the demand

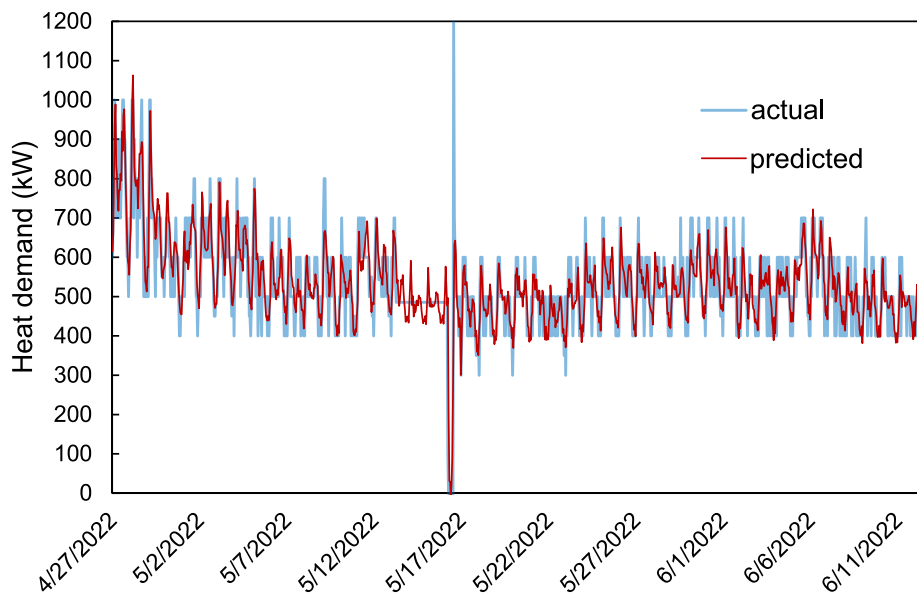


Fig. 12. 12-h ahead demand prediction by LSTM.

in the substation under consideration.

LSTM, as confirmed in related papers [69–71] focusing on building energy forecasting, demonstrated similar performance in our results. These findings underscore the effectiveness of machine learning-based methods for DH demand prediction. In our study, LSTM was selected as the predictive model due to its strong compatibility with MPC [72].

Fig. 12 illustrates the comprehensive 12-h ahead forecasting accuracy of the recursive strategy employing LSTM. The CVRMSE for the validation stands at 11.8%. Although this error is slightly higher than the one-step ahead prediction, the studies [53,72,73] have established that a CVRMSE of approximately 30% or less is acceptable for practical engineering applications. Notably, the observed prediction result falls well below this threshold, indicating the strong accuracy of the multiple steps ahead demand prediction achieved by the proposed LSTM network.

MPC determines optimal control trajectories using predictive mathematical models. Traditional physics-based models require detailed system knowledge and are impractical for large-scale applications like district heating systems. In contrast, machine learning models, such as those discussed earlier (SVR, regression tree, and LSTM), are trained on data and can predict building dynamics without detailed physical information. Therefore, machine learning offers a promising solution for constructing MPC in complex systems, enabling efficient and accurate demand forecasting and control [74–77].

#### 4.2. Model predictive control (MPC) of seasonal thermal energy storage

This section compared the seasonal thermal energy storage capacity without considering the chemical reaction process of the storage system. In another word, this presents the results of the seasonal storage system with immediate heat charge and discharge ignoring the heat loss. The results indicate that different supply scenarios necessitate varying maximal storage capacities. Simulations were conducted for storage capacities ranging from 1000 MWh to 100 MWh, in decrements of 50 MWh. The optimal storage capacities identified for the 80%, 60%, and

Table 3

Performance of different supply scenarios under proposed control strategy.

Supply capacity (based on original scenario)	80%	60%	50%
Waste heat (%)	4%	0%	0%
Unmet heat demand (%)	1%	10%	24%

50% supply scenarios were 1000 MWh, 400 MWh, and 150 MWh, respectively. The corresponding waste heat and unmet heat demand percentages are detailed in Table 3.

For the 80% supply capacity scenario, nearly all stored heat energy was utilized to meet periods of insufficient demand. However, this was not the case for the 60% and 50% scenarios, where stored heat energy was inadequate to fully cover the demand shortfalls.

Fig. 13 illustrates the results for the MPC control strategy under different supply scenarios. The “Storage amount” indicates the rate of heat change in the storage system. “Mismatch” represents the difference between the supply heat amount and the heat load, while “Storage” shows energy being fed into (positive values) and supplied from (negative values) the storage system. During warm months, the supply amount often exceeds the demand, resulting in excess energy being stored. Conversely, in cold months, the heat load might surpass the supply rate, particularly under reduced supply capacity scenarios. This highlights the necessity of a well-sized storage capacity to accommodate seasonal variations in supply and demand. The storage capacity is significantly larger than the hourly supply and demand rates due to the need to store surplus energy generated during warm months for use during cold months. This ensures that the system can effectively balance supply and demand, even when the supply capacity is reduced.

The storage tank is typically charged before a significant mismatch, such as during summer peaks, with heat storage preparation starting around three months in advance. For example, heat stored from June can be used in October (Fig. 13). This approach aligns with the study of [75] where a calcium sulfoaluminate cement seasonal heat storage system was charged with energy during the summer and successfully discharged heat during the winter. The proposed MPC strategy effectively eliminates waste heat from periods of excess heat production and utilizes stored heat during periods of insufficient supply. This ensures efficient energy use and highlights the system's capability to manage seasonal supply and demand variations based on the amount of waste heat stored from the summer.

MPC has demonstrated its capability to effectively shift energy seasonally in all examined cases. With the installation of the proposed STES system, there is a noticeable reduction in the need for auxiliary heating during winter and a decrease in waste heat during summer. We evaluated the energy performance of the STES under various assumed lower supply capacities and their corresponding storage capacities. The findings indicate that the STES system, under MPC control, could manage a 20% lower supply capacity while only resulting 4% of waste

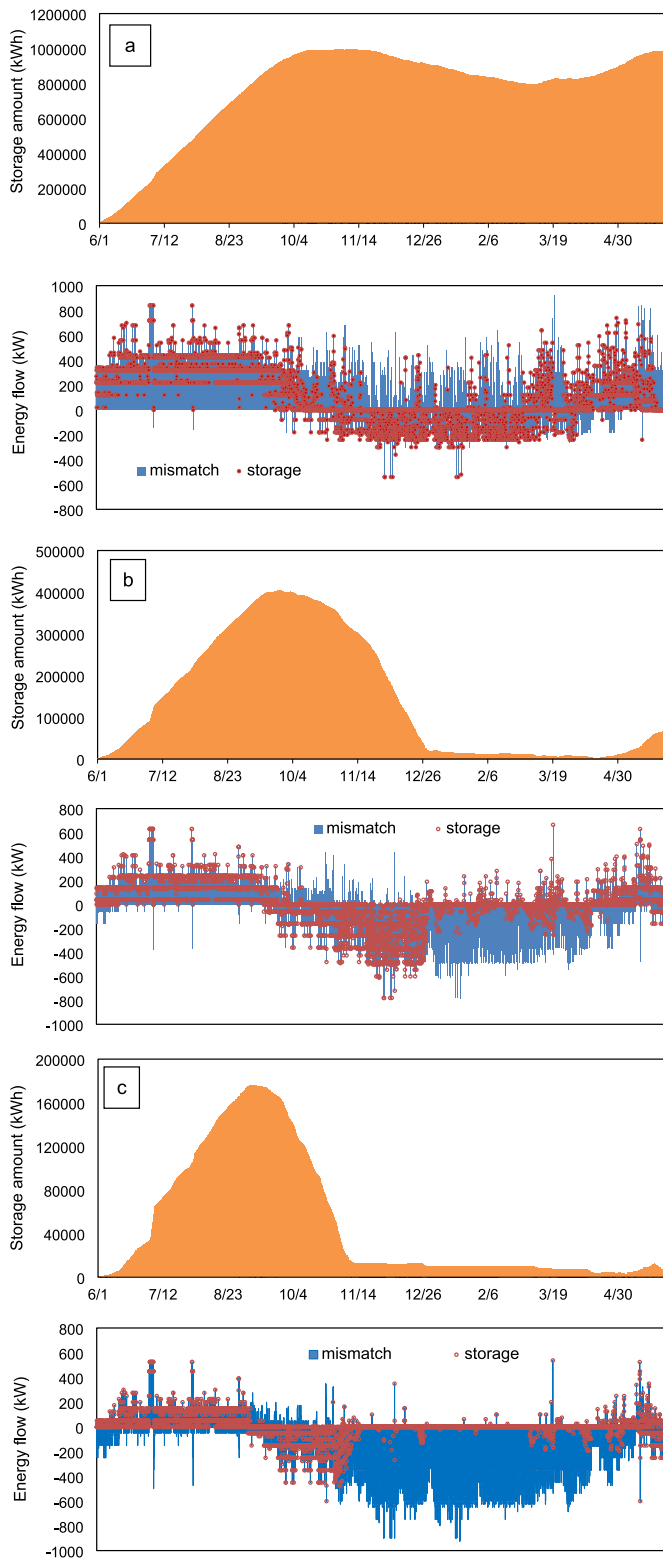


Fig. 13. Storage performance with (a) 80% supply capacity, (b) 60% supply capacity, and (c) 50% supply capacity.

heat and meeting 99% of the total heat demand for the case study substation. However, further reductions in supply capacity revealed that the stored waste heat could not fully meet the heat demand during the cold months. The results are consistent with those found in [76], which demonstrated that the proposed STES system could save up to 60% of energy.

It is important to develop the MPC with appropriate weighting parameters for optimizing STES performance. Additionally, proper formulation can enhance the control and efficiency of seasonal energy storage systems and should be explored further in future studies. Although this study did not explore the integration of renewable energy sources, typically, STES systems are feasible and robust with a stable and sufficient renewable energy sources supply [77]. However, the variable nature of heat sources in STES poses challenges in matching renewable energy sources supply with heat demand using conventional control strategies. Future work could investigate how accurate predictions of RES and heat demand, along with proper sizing of the long-term storage system, could allow MPC to increase RES penetration in district heating grids by mitigating hourly or daily mismatches [6].

With regards to the optimization problem solved, most computation times on a PC with an Intel Core i5-10300H 2.50 GHz processor took less than one second, which is significantly faster than the minimum prediction interval of one hour. This ensures that the MPC controller can perform online control effectively. The proposed MPC implementation allowed all decision information for seasonal storage charging and discharging to be accessible within the prediction horizon of the first control identification for the current year. Additionally, incorporating reference tracking into the objective function by introducing slack variables helps reduce the possibility of processing errors. This adjustment can potentially lower operating costs and significantly reduce computation time in practical applications [47].

#### 4.3. Comparison between model predictive control (MPC) and rule-based control

This section presents the comparison of the results of MPC and a rule-based control strategy, controlling the proposed TCES by taking chemical reactions into account, aiming to determine the extent to which receding horizon optimization outperforms pre-defined rules in long-term decision-making processes. Both control strategies, based on machine learning predictions, successfully shift energy from warm months to winter. Given the highly stochastic nature of demand in DH, accurate demand prediction is crucial. Our results confirmed the direct impact of accurate predictions on storage performance. Simulations were based on the 80% supply capacity scenario, starting from April 27.

Compared to rule-based control, MPC demonstrated improved performance in solving for the optimal inlet temperature (Fig. 14a). Overall, the rule-based control strategy stored 17.2% of waste heat and supplied 27.4% of the total additional heat demand that was not covered by the auxiliary heat supply. In contrast, MPC stored 99.6% of waste heat and supplied 85.2% of the additional heat demand, showing its effectiveness in optimizing energy use and meeting heat demand more efficiently.

Fig. 15a illustrates how the MPC strategy effectively minimizes the mismatch between the heat supply rate and heat loads (“mismatch” in Fig. 15a). Blue points mean surplus/shortfall in heat supply before the implementation of the MPC strategy. Red points are showing that MPC are trying to cover all surplus/shortfall heat by storing/releasing heat into/from TCES. MPC is not able to cover the blue points towards the end as there is not heat stored in TCES at that time. Overall, MPC controlled TCES can provide 85% of the additional heat demand by storing 99% waste heat.

Here, “surplus” (positive) indicates the waste heat generated from excess heat production, while “insufficient” (negative) denotes the shortfall in heat required to meet demand. Fig. 15b presents the mismatch between the DH heat supply, coupled with the TCES system, and heat loads after implementing the two control strategies. “Waste heat” (positive) indicates the heat that was neither stored by the TCES nor utilized by the demand side. “Insufficient” (negative) represents the heat shortfall that could not meet the heat loads, even when using both the stored heat from the TCES and the supply from the heat station. It is evident that rule-based control often struggles to reduce waste heat while meeting DH demand (Fig. 15b). This approach cannot ensure both

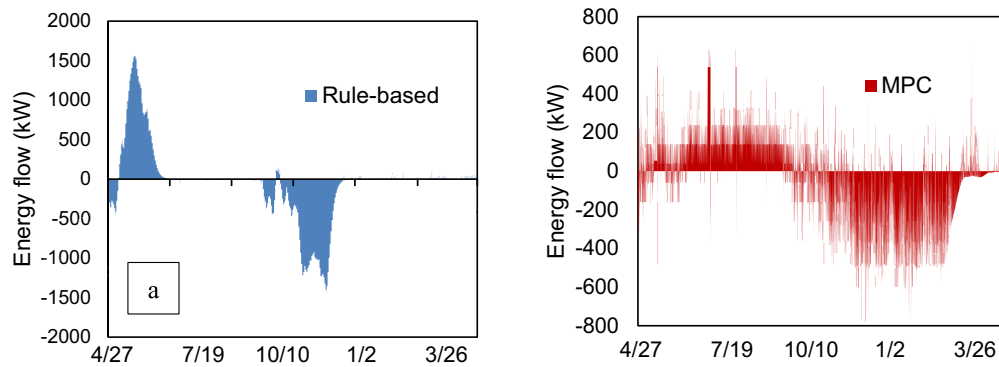


Fig. 14. Energy storage flow comparison under (a) rule-based strategy, and (b) MPC strategy.

the reduction of waste heat and adequate energy supply when demand exceeds capacity, as it lacks the ability to manage system disturbances effectively. In contrast, MPC optimizes energy storage and maintains compliance with constraints, utilizing prediction models to accurately manage and respond to system disturbances.

Fig. 15(c) illustrates the transition of  $\text{Co}_3\text{O}_4/\text{CoO}$  over a year under the MPC strategy, with different lines indicating the amount of  $\text{Co}_3\text{O}_4$  in the TCES at various temperature nodes from the inlet to the outlet. In the initial months,  $\text{Co}_3\text{O}_4$  levels peak, indicating effective heat absorption during the charging phase. This is followed by a stable period, signifying the stability of the stored heat until the temperature drops enough to initiate the oxidation reaction. During the colder months, the amount of  $\text{Co}_3\text{O}_4$  decreases, showing the discharge of stored chemical and sensible heat. However, several limitations exist. Complete conversion of  $\text{Co}_3\text{O}_4$  to  $\text{CoO}$  and vice versa is unlikely due to inefficiencies and incomplete reactions, leaving residual  $\text{Co}_3\text{O}_4$  at full discharge. Operational constraints such as temperature fluctuations, pressure variations, and material degradation over time can impact TCES system efficiency and performance.

The use of MPC in district heating systems demonstrates advantages in managing the complexities and fluctuations of thermal loads. Operating DH systems with variable loads presents a challenging task that necessitates control strategies capable of handling thermal energy storage, flexible loads, and operational constraints [78]. The results showed that MPC optimizes thermal energy storage, reduces waste heat, and meets energy demands more efficiently than traditional rule-based controls. By integrating predictive models, our study highlights MPC's improved system performance and adaptability under various supply conditions, emphasizing its potential for large-scale district heating networks. These findings support the further exploration and adoption of MPC to enhance the efficiency and sustainability of district heating systems.

## 5. Conclusion and future works

This research has explored the integration of MPC with seasonal thermochemical energy storage systems (STES) within the context of district heating networks, focusing on the Nottingham district heating as a case study. Our primary objective was to develop an intelligent MPC strategy that employs machine learning models for accurate heat load forecasting and optimizes the charging and discharging cycles of thermochemical energy storage systems.

The method employed in this study utilized and validated machine learning models, including support vector regression (SVR), regression trees, and long short-term memory (LSTM) networks, for accurate heat load prediction based on historical heat load and meteorological data. A numerical model of the thermochemical energy storage system (TCES) was adopted and validated with experimental data. This TCES model was integrated into the MPC framework, formulated as a mixed-integer linear program, to optimize the charging and discharging cycles of the

STES. The MPC strategy's performance was compared with a traditional rule-based control approach, and various supply capacities were tested to assess its scalability and robustness. Computational efficiency was evaluated to ensure practical real-time control applicability.

Each machine learning model demonstrated comparable performance, with CVRMSE values within the 9–11% range. The LSTM model excelled in handling sequential data, providing accurate multi-step forecasts crucial for the MPC framework. Incorporating these models into the MPC strategy enabled precise heat demand predictions, enhancing the control of energy storage and distribution. This highlights the vital role of machine learning in optimizing district heating systems.

The MPC strategy outperformed the traditional rule-based control approach. Simulations indicated that MPC could efficiently store surplus heat during low-demand periods and utilize it during high-demand periods, reducing overall waste heat and meeting heating demands more effectively. Specifically, the MPC strategy managed to store 99.6% of waste heat and meet 85.2% of the total additional heat demand that was not covered by the auxiliary heat supply, compared to the rule-based control's 17.2% and 27.4%, respectively. This emphasizes MPC's capability in optimizing energy storage and distribution within district heating networks.

The results demonstrated that the system could accommodate reductions in supply capacity to a certain extent, but performance degraded beyond specific thresholds. For instance, at 80% supply capacity, the system efficiently utilized stored heat to meet demand. However, at 50% capacity, the stored waste heat was insufficient to cover the entire demand during colder months. These insights are crucial for planning and scaling district heating systems with integrated STES, emphasizing the need for careful consideration of supply capacities in system design.

The MPC optimization problem was computationally efficient, with most computations taking less than a second on a standard PC, making it viable for real-time control applications. This rapid computation capability ensures the MPC can adjust to changing conditions and maintain optimal performance in dynamic environments.

Our study has shown the potential of machine learning models with MPC to enhance the performance and adaptability of district heating systems with STES under varying supply conditions. The MPC strategy effectively manages energy storage and distribution, minimizing waste heat and efficiently meeting energy demands. This adaptability is essential for large-scale networks with fluctuating demand and supply. The findings support wider adoption of MPC in district heating systems for energy savings and emission reductions, aligning with global carbon neutrality goals.

Despite the promising results, several limitations should be acknowledged. The study did not integrate renewable energy sources (RES) into the DH network, which could offer additional benefits and challenges. The accuracy of machine learning models depends on high-quality historical data and may be affected by data anomalies. The simulations, based on a specific case study in Nottingham, may yield

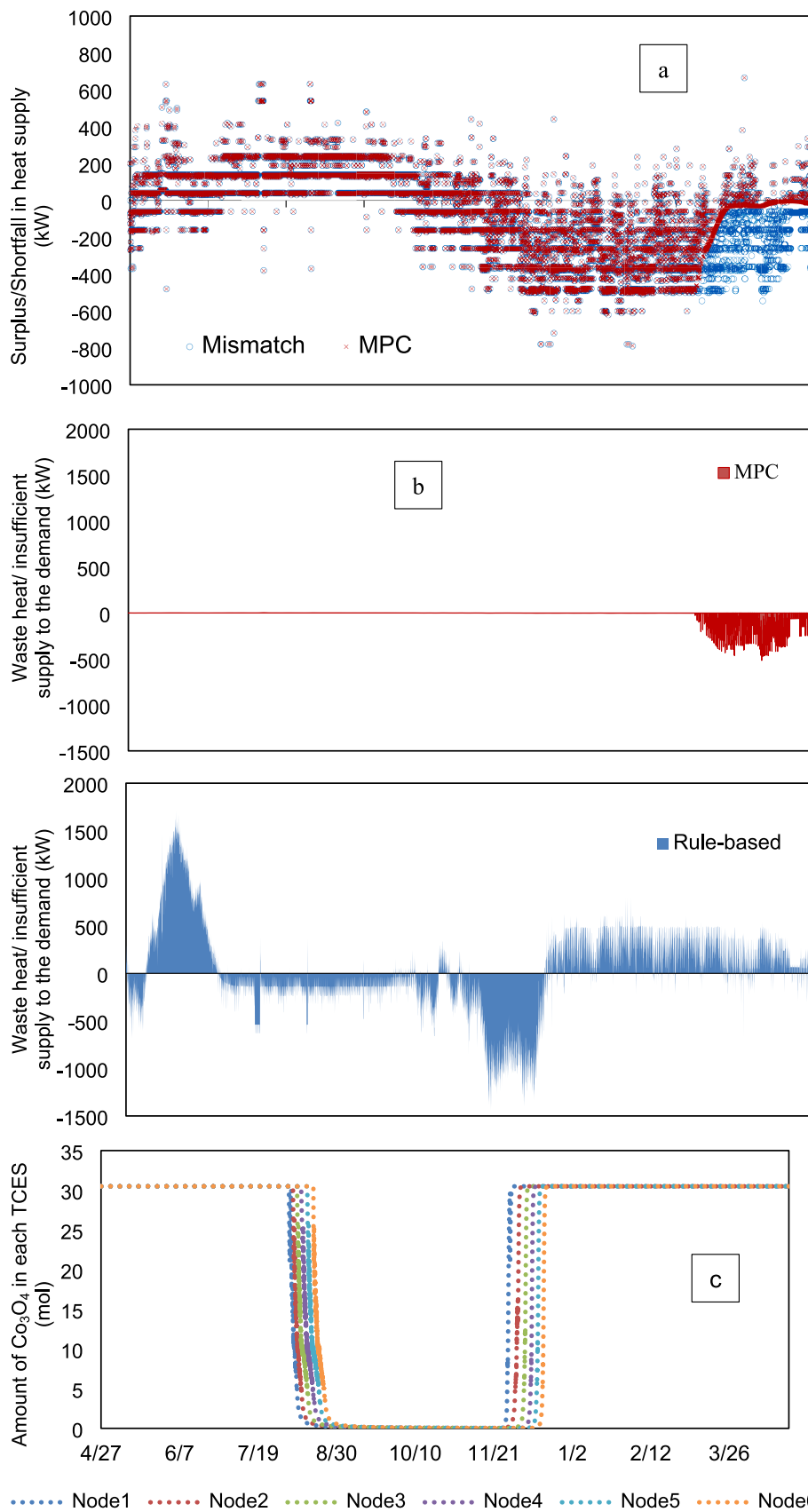


Fig. 15. (a) The MPC strategy addressing the mismatch between the heat supply rate and heat loads, (b) mismatch between DH heat supply (coupled with TCES) and heat loads after implementing two control strategies, and (c) amount of  $\text{Co}_3\text{O}_4$  in TCES under MPC control.

different results in other locations or DH configurations. Lastly, larger and more complex DH systems might require further optimization of the MPC algorithms to maintain real-time performance.

Future research should prioritize integrating renewable energy sources with STES in district heating networks to enhance performance and sustainability. Additionally, exploring diverse heat sources can significantly improve the system's flexibility and resilience. Further refinement of MPC strategies, including appropriate weighting parameters, is essential for optimization. Additionally, investigating different types of TCES systems with various materials will provide insights into their efficiency. Practical challenges and solutions for implementing MPC and STES in real-world networks should be investigated to ensure scalability and robustness. Extensive simulations and real-world case studies are crucial for further validation.

#### CRediT authorship contribution statement

**Zhichen Wei:** Writing – original draft, Validation, Software, Methodology, Investigation, Formal analysis, Conceptualization. **Paige Wenbin Tien:** Data curation. **John Calautit:** Supervision. **Jo Darkwa:** Supervision. **Mark Worall:** Supervision. **Rabah Boukhanouf:** Supervision.

#### Declaration of competing interest

The authors declare that they have no known competing financial interests or personal relationships that could have appeared to influence the work reported in this paper.

#### Data availability

Data will be made available on request.

#### Acknowledgements

The authors would like to acknowledge the Engineering and Physical Sciences Research Council (EPSRC), UK for funding the research under Grant No EP/V041452/1 (VTTESS- Variable-Temperature Thermochemical Energy Storage System and Heat Networks for Decarbonising the Buildings Sector).

#### References

- [1] IEA. Transition to sustainable buildings [electronic resource]: Strategies and opportunities to 2050 / IEA (transition to sustainable buildings). Paris: Paris: IEA; 2013.
- [2] Goodright V. "Estimates of heat use in the United Kingdom in 2013," DECC Statistics. 2014.
- [3] Mahon D, Henshall P, Claudio G, Eames PC. Feasibility study of MgSO<sub>4</sub> + zeolite based composite thermochemical energy stores charged by vacuum flat plate solar thermal collectors for seasonal thermal energy storage. *Renew Energy* 2020;145: 1799–807. <https://doi.org/10.1016/j.renene.2019.05.135>.
- [4] Yeh C-Y, De Swart JK, Mahmoudi A, Singh AK, Brem G, Shahi M. Simulation-based analysis of thermochemical heat storage feasibility in third-generation district heating systems: case study of Enschede. *Netherlands Renewable Energy* 2024;221: 119734. <https://doi.org/10.1016/j.renene.2023.119734>.
- [5] Roger-Lund S, Darkwa J, Worall M, Calautit J, Boukhanouf R. A review of thermochemical energy storage systems for district heating in the UK. *Energies* 2024;17:3389. <https://doi.org/10.3390/en17143389>.
- [6] Renaldi R, Friedrich D. Techno-economic analysis of a solar district heating system with seasonal thermal storage in the UK. *Appl Energy* 2019;236:388–400. <https://doi.org/10.1016/j.apenergy.2018.11.030>.
- [7] Kur A, Darkwa J, Calautit J, Boukhanouf R, Worall M. Solid-Gas thermochemical energy storage materials and reactors for low to high-temperature applications: A concise review. *Energies* 2023;16:756. <https://doi.org/10.3390/en16020756>.
- [8] Alkhalidi A, Al Khatba H, Khawaja MK. Utilization of Buildings' foundations for a seasonal thermal energy storage medium to meet space and water heat demands. *International Journal of Photoenergy* 2021;2021:1–17. <https://doi.org/10.1155/2021/6668079>.
- [9] Li T, Wang R, Kiplagat JK, Kang Y. Performance analysis of an integrated energy storage and energy upgrade thermochemical solid-gas sorption system for seasonal storage of solar thermal energy. *Energy (Oxford)* 2013;50:454–67. <https://doi.org/10.1016/j.energy.2012.11.043>.
- [10] Yang T, Liu W, Sun Q, Hu W, Kramer GJ. Techno-economic-environmental analysis of seasonal thermal energy storage with solar heating for residential heating in China. *Energy* 2023;283:128389. <https://doi.org/10.1016/j.energy.2023.128389>.
- [11] Benzama MH, Menhoudj S, Lekhal MC, Mokhtari A, Attia S. Multi-objective optimisation of a seasonal solar thermal energy storage system combined with an earth – air heat exchanger for net zero energy building. *Sol Energy* 2021;220: 901–13. <https://doi.org/10.1016/j.solener.2021.03.070>.
- [12] Schrader AJ, De Dominicis G, Schieber GL, Loutzenhiser PG. Solar electricity via an air Brayton cycle with an integrated two-step thermochemical cycle for heat storage based on Co<sub>3</sub>O<sub>4</sub>/CoO redox reactions III: solar thermochemical reactor design and modeling. *Sol Energy* 2017;150(C):584–95. <https://doi.org/10.1016/j.solener.2017.05.003>.
- [13] Pardo P, Deydier A, Anxionnaz-Minvielle Z, Rougé S, Cabassud M, Cognet P. A review on high temperature thermochemical heat energy storage. *Renew Sust Energy Rev* 2014;32:591–610. <https://doi.org/10.1016/j.rser.2013.12.014>.
- [14] Tesfari S, Lantin G, Lange M, Breuer S, Agrafiotis C, Roeb M, et al. Numerical model to design a thermochemical storage system for solar power plant. *Energy Procedia* 2015;75:2137–43. <https://doi.org/10.1016/j.egypro.2015.07.347>.
- [15] Wong B. Thermochemical heat storage for concentrated solar power: General atomics report GA-C271372011 for the U.S. San Diego, CA, U.S.A: Department of Energy; 2011. <http://www.osti.gov/scitech/biblio/1039304/> [accessed on 05/16/2024].
- [16] Singh A, Tesfari S, Lantin G, Agrafiotis C, Roeb M, Sattler C. Solar thermochemical heat storage via the Co<sub>3</sub>O<sub>4</sub>/CoO looping cycle: storage reactor modelling and experimental validation. *Sol Energy* 2017;144:453–65. <https://doi.org/10.1016/j.solener.2017.01.052>.
- [17] Li Z, Xu M, Huai X, Huang C, Wang K. Simulation and analysis of thermochemical seasonal solar energy storage for district heating applications in China. *Int J Energy Res* 2021;45(5):7093–107. <https://doi.org/10.1002/er.6295>.
- [18] Chen C, Aryafar H, Lovegrove KM, Lavine AS. Modeling of ammonia synthesis to produce supercritical steam for solar thermochemical energy storage. *Sol Energy* 2017;155(C):363–71. <https://doi.org/10.1016/j.solener.2017.06.049>.
- [19] Han X, Wang L, Ling H, Ge Z, Lin X, Dai X, et al. Critical review of thermochemical energy storage systems based on cobalt, manganese, and copper oxides. *Renew Sust Energy Rev* 2022;158:112076. <https://doi.org/10.1016/j.rser.2022.112076>.
- [20] Mohapatra D, Nandanavanam J. Salt in matrix for thermochemical energy storage - A review. *Materials Today: Proceedings* 2023;72:27–33. <https://doi.org/10.1016/j.matpr.2022.05.453>.
- [21] Nagamani G, Naik BK, Agarwal S. Energetic and exergetic performance analyses of mobile thermochemical energy storage system employing industrial waste heat. *Energy* 2024;288:129730. <https://doi.org/10.1016/j.energy.2023.129730>.
- [22] Böhm H, Lindorfer J. Techno-economic assessment of seasonal heat storage in district heating with thermochemical materials. *Energy* 2019;179:1246–64. <https://doi.org/10.1016/j.energy.2019.04.177>.
- [23] Li TX, Wang RZ, Yan T, Ishugah TF. Integrated energy storage and energy upgrade, combined cooling and heating supply, and waste heat recovery with solid-gas thermochemical sorption heat transformer. *Int J Heat Mass Transf* 2014;76: 237–46. <https://doi.org/10.1016/j.ijheatmasstransfer.2014.04.046>.
- [24] Li T, Wang R, Kiplagat JK. A target-oriented solid-gas thermochemical sorption heat transformer for integrated energy storage and energy upgrade. *AIChE J* 2013; 59(4):1334–47. <https://doi.org/10.1002/aic.13899>.
- [25] Mastronardo E, Kato Y, Bonaccorsi L, Piperopoulos E, Milone C. Thermochemical storage of middle temperature wasted heat by functionalized C/mg(OH)<sub>2</sub> hybrid materials. *Energies* 2017;10(1):70. <https://doi.org/10.3390/en10010070>.
- [26] Gao P, Wei X, Wang L, Zhu F. Compression-assisted decomposition thermochemical sorption energy storage system for deep engine exhaust waste heat recovery. *Energy (Oxford)* 2022;244:123215. <https://doi.org/10.1016/j.energy.2022.123215>.
- [27] Gao P, Wang LW, Zhu FQ. Vapor-compression refrigeration system coupled with a thermochemical resorption energy storage unit for a refrigerated truck. *Appl Energy* 2021;290:116756. <https://doi.org/10.1016/j.apenergy.2021.116756>.
- [28] Yan T, Zhang H, Yu N, Li D, Pan QW. Performance of thermochemical adsorption heat storage system based on MnCl<sub>2</sub>-NH<sub>3</sub> working pair. *Energy (Oxford)* 2022;239: 122327. <https://doi.org/10.1016/j.energy.2021.122327>.
- [29] Weber SO, Oei M, Linder M, Böhm M, Leistner P, Sawodny O. Model predictive approaches for cost-efficient building climate control with seasonal energy storage. *Eng Buildings* 2022;270:112285. <https://doi.org/10.1016/j.enbuild.2022.112285>.
- [30] Tesfari S, Singh A, Agrafiotis C, de Oliveira L, Breuer S, Schlögl-Knothe B, et al. Experimental evaluation of a pilot-scale thermochemical storage system for a concentrated solar power plant. *Appl Energy* 2017;189:66–75. <https://doi.org/10.1016/j.apenergy.2016.12.032>.
- [31] International Energy Agency. Technology roadmap—Energy storage. *International Energy Agency*: Paris, France; 2014.
- [32] Gufo-Pérez DC, Martínez Castilla G, Pallarès D, Thunman H, Johnsson F. Thermochemical energy storage with Integrated District heat production—a case study of Sweden. *Energies (Basel)* 2023;16(3):1155. <https://doi.org/10.3390/en16031155>.
- [33] Bayon A, Bader R, Jafarian M, Fedunik-Hofman L, Sun Y, Hinkley J, et al. Techno-economic assessment of solid-gas thermochemical energy storage systems for solar thermal power applications. *Energy (Oxford)* 2018;149:473–84. <https://doi.org/10.1016/j.energy.2017.11.084>.
- [34] Lepiksaar K, Masatin V, Latšov E, Sirdre A, Volkova A. Improving CHP flexibility by integrating thermal energy storage and power-to-heat technologies into the energy system. *Smart Energy (Amsterdam)* 2021;2:100022. <https://doi.org/10.1016/j.segy.2021.100022>.

- [35] Jimenez-Navarro J-P, Kavvadias K, Filippidou F, Pavičević M, Quoilin S. Coupling the heating and power sectors: the role of centralised combined heat and power plants and district heat in a European decarbonised power system. *Appl Energy* 2020;270:115134. <https://doi.org/10.1016/j.apenergy.2020.115134>.
- [36] Johar DK, Sharma D, Soni SL. Comparative studies on micro cogeneration, micro cogeneration with thermal energy storage and micro trigeneration with thermal energy storage system using same power plant. *Energy Convers Manag* 2020;220:113082. <https://doi.org/10.1016/j.enconman.2020.113082>.
- [37] Li X, Wang Z, Li J, Yang M, Yuan G, Bai Y, et al. Comparison of control strategies for a solar heating system with underground pit seasonal storage in the non-heating season. *J Energy Storage* 2019;26:100963. <https://doi.org/10.1016/j.est.2019.100963>.
- [38] Labidi M, Eynard J, Faugeroux O, Grieu S. A new strategy based on power demand forecasting to the management of multi-energy district boilers equipped with hot water tanks. *Appl Therm Eng* 2017;113:1366–80. <https://doi.org/10.1016/j.applthermaleng.2016.11.151>.
- [39] Jonin M, Khosravi M, Eichler A, Villasmil W, Schuetz P, Jones CN, et al. Exergy-based model predictive control for design and control of a seasonal thermal energy storage system. *J Phys Conf Ser* 2019;1343(1):12066. <https://doi.org/10.1088/1742-6596/1343/1/012066>.
- [40] Milewski J, Szabłowski Łukasz, Bujalski W. Identification of the objective function for optimization of a seasonal thermal energy storage system. *Archives of Thermodynamics* 2014;35(4):69–81. <https://doi.org/10.2478/aoter-2014-0034>.
- [41] Rostampour V, Keviczky T. Probabilistic energy Management for Building Climate Comfort in smart thermal grids with seasonal storage systems. *IEEE Transactions on Smart Grid* 2019;10(4):3687–97. <https://doi.org/10.1109/TSG.2018.2834150>.
- [42] Saloux E, Candanedo JA. Model-based predictive control to minimize primary energy use in a solar district heating system with seasonal thermal energy storage. *Appl Energy* 2021;291:116840. <https://doi.org/10.1016/j.apenergy.2021.116840>.
- [43] Lago J, Suryanarayana G, Sogancioglu E, De Schutter B. Optimal control strategies for seasonal thermal energy storage systems with market interaction. *IEEE Trans Control Syst Technol* 2021;29(5):1891–906. <https://doi.org/10.1109/TCST.2020.3016077>.
- [44] Dotzauer E. Simple model for prediction of loads in district-heating systems. *Appl Energy* 2002;73(3):277–84. [https://doi.org/10.1016/S0306-2619\(02\)00078-8](https://doi.org/10.1016/S0306-2619(02)00078-8).
- [45] Fang T, Lahdelma R. Evaluation of a multiple linear regression model and SARIMA model in forecasting heat demand for district heating system. *Appl Energy* 2016;179:544–52. <https://doi.org/10.1016/j.apenergy.2016.06.133>.
- [46] Idowu S, Saguna S, Åhlund C, Schelén O. Applied machine learning: forecasting heat load in district heating systems. *Energy Buildings* 2016;133:478–88. <https://doi.org/10.1016/j.enbuild.2016.09.068>.
- [47] Xue P, Jiang Y, Zhou Z, Chen X, Fang X, Liu J. Multi-step ahead forecasting of heat load in district heating systems using machine learning algorithms. *Energy (Oxford)* 2019;188:116085. <https://doi.org/10.1016/j.energy.2019.116085>.
- [48] Grosswindhagera S, Voigtb A, Kozeka M. Online short-term forecast of system heat load in district heating networks. *Tsp* 2011;1(2):1–8. <http://hdl.handle.net/20.500.12708/66419>.
- [49] Wang M, Tian Q. Application of wavelet neural network on thermal load forecasting. *Int J Wirel Mob Comput* 2013;6(6):608–14. <https://doi.org/10.1504/IJWMC.2013.057579>.
- [50] Géron A. *Hands-on machine learning with Scikit-learn and TensorFlow*. 1st ed. Incorporated: O'Reilly Media; 2017.
- [51] Wu, L., Kaiser, G., Solomon, D., Winter, R., Boulanger, A., & Anderson, R. (2012). Improving efficiency and reliability of building systems using machine learning and automated online evaluation. 2012 IEEE Long Island systems, applications and technology conference (LISAT), 1–6. Doi: <https://doi.org/10.1109/LISAT.2012.6223192>.
- [52] Catalina T, Iordache V, Caracaleanu B. Multiple regression model for fast prediction of the heating energy demand. *Energy Buildings* 2013;57:302–12. <https://doi.org/10.1016/j.enbuild.2012.11.010>.
- [53] Edwards RE, New J, Parker LE. Predicting future hourly residential electrical consumption: a machine learning case study. *Energy Buildings* 2012;49:591–603. <https://doi.org/10.1016/j.enbuild.2012.03.010>.
- [54] Safavian SR, Landgrebe D. A survey of decision tree classifier methodology. *IEEE Trans Syst Man Cybern* 1991;21(3):660–74. <https://doi.org/10.1109/21.97458>.
- [55] Potočník P, Škerl P, Govekar E. Machine-learning-based multi-step heat demand forecasting in a district heating system. *Energy Buildings* 2021;233:110673. <https://doi.org/10.1016/j.enbuild.2020.110673>.
- [56] Huang K, Wei K, Li F, Yang C, Gui W. LSTM-MPC: a deep learning based predictive control method for multimode process control. *IEEE Transactions on Industrial Electronics (1982)* 2023;70(11):11544–54. <https://doi.org/10.1109/TIE.2022.3229323>.
- [57] Matlab S. *Matlab*. Natick, MA: The MathWorks; 2012.
- [58] Pagkoura C, Karagiannakis G, Halevas E, Konstandopoulos AG. Co3O4-based honeycombs as compact redox reactors/heat exchangers for thermochemical storage in the next generation CSP plants. AIP Conference Proceedings 2016;1734(1). <https://doi.org/10.1063/1.4949135>.
- [59] Zhou X, Mahmood M, Chen J, Yang T, Xiao G, Ferrari ML. Validated model of thermochemical energy storage based on cobalt oxides. *Appl Therm Eng* 2019;159:113965. <https://doi.org/10.1016/j.applthermaleng.2019.113965>.
- [60] Huber ML, Lemmon EW, Bell IH, McLinden MO. The NIST REFPROP database for highly accurate properties of industrially important fluids. *Ind Eng Chem Res* 2022;61(42):15449–72. <https://doi.org/10.1021/acs.iecr.2c01427>.
- [61] Lofberg J. "YALMIP: A toolbox for modeling and optimization in MATLAB," in 2004 IEEE international conference on robotics and automation (IEEE Cat. No. 04CH37508). 2004. <https://doi.org/10.1109/CACSD.2004.1393890>. IEEE, pp. 284–289.
- [62] Bixby B. The *gurobi* optimizer. *Transp Re-search Part B* 2007;41(2):159–78.
- [63] Romanchenko D, Kensby J, Odenberger M, Johansson F. Thermal energy storage in district heating: centralised storage vs. storage in thermal inertia of buildings. *Energy Convers Manag* 2018;162:26–38. <https://doi.org/10.1016/j.enconman.2018.01.068>.
- [64] Peng Y, Rysanek A, Nagy Z, Schlüter A. Using machine learning techniques for occupancy-prediction-based cooling control in office buildings. *Appl Energy* 2018;211:1343–58. <https://doi.org/10.1016/j.apenergy.2017.12.002>.
- [65] Saletti C, Gambarotta A, Morini M. Development, analysis and application of a predictive controller to a small-scale district heating system. *Appl Therm Eng* 2020;165:114558. <https://doi.org/10.1016/j.applthermaleng.2019.114558>.
- [66] Jansen J, Jorissen F, Helsen L. Mixed-integer non-linear model predictive control of district heating networks. *Appl Energy* 2024;361. <https://doi.org/10.1016/j.apenergy.2024.122874>.
- [67] Manente G, Lazzaretto A, Molinari I, Bronzini F. Optimization of the hydraulic performance and integration of a heat storage in the geothermal and waste-to-energy district heating system of Ferrara. *J Clean Prod* 2019;230:869–87. <https://doi.org/10.1016/j.jclepro.2019.05.146>.
- [68] Chen S, Lior N, Xiang W. Coal gasification integration with solid oxide fuel cell and chemical looping combustion for high-efficiency power generation with inherent CO<sub>2</sub> capture. *Appl Energy* 2015;146:298–312. <https://doi.org/10.1016/j.apenergy.2015.01.100>.
- [69] Gao Y, Fang C, Ruan Y. A novel model for the prediction of long-term building energy demand: LSTM with attention layer. *IOP conference series. Earth and environmental. Science* 2019;294(1):12033. <https://doi.org/10.1088/1755-1315/294/1/012033>.
- [70] Jang J, Han J, Leigh S-B. Prediction of heating energy consumption with operation pattern variables for non-residential buildings using LSTM networks. *Energy Buildings* 2022;255:111647. <https://doi.org/10.1016/j.enbuild.2021.111647>.
- [71] Fang Z, Crimier N, Scanu L, Midelet A, Alyafi A, Delinchant B. Multi-zone indoor temperature prediction with LSTM-based sequence to sequence model. *Energy Buildings* 2021;245:111053. <https://doi.org/10.1016/j.enbuild.2021.111053>.
- [72] Huang K, Wei K, Li F, Yang C, Gui W. LSTM-MPC: a deep learning based predictive control method for multimode process control. *IEEE Transactions on Industrial Electronics (1982)* 2023;70(11):11544–54. <https://doi.org/10.1109/TIE.2022.3229323>.
- [73] Reddy TA, Maor I, Panjapornpon C. Calibrating detailed building energy simulation programs with measured data-part II: application to three case study office buildings (RP-1051). *HVAC&R Research* 2007;13(2):243–65. <https://doi.org/10.1080/10789669.2007.10390953>.
- [74] Henze GP. Model predictive control for buildings: a quantum leap? *J Build Perform Simul* 2013;6(3):157–8. <https://doi.org/10.1080/19401493.2013.778519>.
- [75] Kaufmann J, Winnefeld F. Seasonal heat storage in calcium sulfoaluminate based hardened cement pastes – experiences with different prototypes. *J Energy Storage* 2019;25:100850. <https://doi.org/10.1016/j.est.2019.100850>.
- [76] Andersson O, Hellström G, Nordell B. Heating and cooling with UTES in Sweden: Current situation and potential market development. In: *International conference on thermal energy storage: 01/09/2003–04/09/2003*. PW Publishing House; 2003. p. 207–15.
- [77] Sibbitt B, McClenahan D, Djebbar R, Thornton J, Wong B, Carriere J, et al. The performance of a high solar fraction seasonal Storage District heating system – five years of operation. *Energy Procedia* 2012;30:856–65. <https://doi.org/10.1016/j.egypro.2012.11.097>.
- [78] Verrilli F, Srinivasan S, Gambino G, Canelli M, Himanka M, Del Vecchio C, et al. Model predictive control-based optimal operations of district heating system with thermal energy storage and flexible loads. *IEEE Trans Autom Sci Eng* 2017;14(2):547–57. <https://doi.org/10.1109/TASE.2016.2618948>.